REPORT DOCUMENTATION PAGE

OMB No. 0704-0188

1. AGENCY USE ONLY (*Leave Blank*)	2. REPORT DATE	3. REPORT TYPE AND DATES COVERED
	14 August 1997	Final Report 15 May 95-14 Aug 97

4. TITLE AND SUBTITLE
The Use of Electrochemistry and Ellipsometry for Identifying and Evaluating Corrosion on Aircraft.

5. FUNDING NUMBERS
Program Solicitation 94-1
Control # 94-NC-133
Contract # F49620-95-C-0040
3005/SS 65502F

6. AUTHOR(S)
Chester M. Dacres, Guy D. Davis, Lorrie A. Krebs, Mark B. Shook

7. PERFORMING ORGANIZATION NAME(S) AND ADDRESS(ES)
DACCO SCI, INC.
10260 Old Columbia Road
Columbia, MD 21046

8. PERFORMING ORGANIZATION REPORT NUMBER
AFOSR-TR-97
0298

9. SPONSORING/MONITORING AGENCY NAME(S) AND ADDRESS(ES)
Air Force Office of Scientific Research (AFOSR)
110 Duncan Avenue
Bolling AFB, DC 20332-0001
NL

AGENCY REPORT NUMBER

11. SUPPLEMENTARY NOTES

12a. DISTRIBUTION/AVAILABILITY STATEMENT
Unrestricted

12b. DISTRIBUTION CODE

19971002 019

13. ABSTRACT (*Maximum 200 words*)

The objective of this SBIR Phase II project (F49620-95-C-0040) was to develop a sensor that could be used by the USAF to monitor the degree of corrosion in aircraft. Electrochemical Impedance Spectroscopy (EIS) has been performed on aluminum alloy samples coated under military specifications. Precise impedance signatures were acquired in order to develop a simple, yet powerful, sensor for the early detection and measurement of corrosion processes on aircraft.

Two versions of prototype sensors have been developed in the Phase II effort to obtain the EIS signature utilizing a two-electrode approach. One version is a portable hand-held unit while the second version is permanently attached. The two-electrode approach enables reliable *in-situ*, real-time analyses of aircraft metal/coating systems under actual service conditions. Results of the Phase II laboratory testing show that the sensors are capable of tracking the corrosion process on the aluminum substrates under a variety of environmental conditions and substrate configurations. Field testing of the portable unit has shown that the technique can be conducted in the field with results comparable to the laboratory.

14. SUBJECT TERMS	15. NUMBER OF PAGES
Aircraft Electrochemistry AC Impedance Electrode Corrosion XPS Ellipsometry Sensors	50
	16. PRICE CODE

17. SECURITY CLASSIFICATION OF REPORT	18. SECURITY CLASSIFICATION OF THIS PAGE	19. SECURITY CLASSIFICATION OF ABSTRACT	20. LIMITATION OF ABSTRACT
Unclassified	Unclassified	Unclassified	UL

PHASE II

FINAL TECHNICAL REPORT

ON

THE USE OF ELECTROCHEMISTRY AND ELLIPSOMETRY FOR IDENTIFYING AND EVALUATING CORROSION ON AIRCRAFT

SMALL BUSINESS INNOVATION RESEARCH (SBIR)
CONTRACT NO. F49620-95-C-0040

Submitted by

Chester M. Dacres
Principal Investigator
DACCO SCI, INC.
10260 Old Columbia Road
Columbia, MD 21046-1218

Submitted to

Major Hugh C. DeLong
Program Manager
AFOSR/NL
110 Duncan Avenue, Suite B115
Bolling AFB, DC 20332-0001

12 August 1997

DSI-AF-9718

TABLE OF CONTENTS

TABLE OF FIGURES

SUMMARY:

The Unites States Air Force (USAF) aircraft fleet is aging and corrosion is becoming increasingly important. The objective of this SBIR Phase II project (F49620-95-C-0040) was to develop a sensor that could be used by the USAF to monitor the degree of aircraft corrosion. Electrochemical corrosion testing using Electrochemical Impedance Spectroscopy (EIS, also known as ac impedance) has been performed on aluminum 2024-T3, 6061-T6, and 7075-T6 samples coated under military specifications. Electrochemical impedance measurements were used to acquire a precise impedance signature which was used to develop a simple, yet powerful, sensor for the early detection and measurement of corrosion processes on aircraft.

The data show that the painted aircraft aluminum 2024-T3, 6061-T6, and 7075-T6 degrade with similar signatures which corresponds to the plot in Figure 1. There are definite regions on the corrosion spectrum showing water uptake, incubation, and intense corrosion activity. The use of ellipsometry and DC electrochemical techniques have verified the results obtained from the EIS technique.

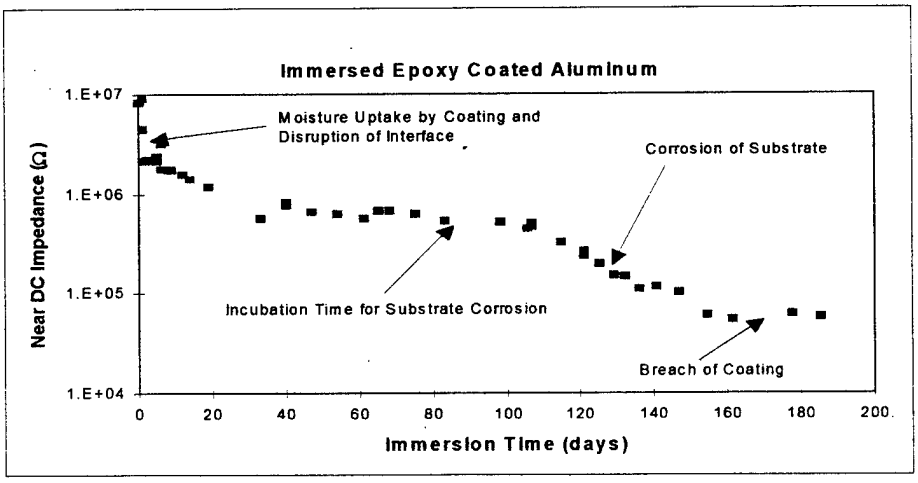

Figure 1. *Typical corrosion process for painted aircraft aluminum.*

Two versions of prototype electrode sensors have been developed in the Phase II effort to obtain this signature utilizing a two-electrode approach. One version is a hand-held, portable unit, while the second version is permanently attached. Conventional EIS requires the use of three electrodes and an electrolyte, making *in-situ* analyses difficult to perform. The two-electrode approach eliminates the need for an electrolyte and enables reliable *in-situ*, real-time analyses of aircraft metal/coating systems under actual service conditions. The results of the Phase II laboratory testing have shown that the sensors are capable of tracking the corrosion process on the aluminum substrates under a variety of temperature and humidity conditions, and on different aircraft substrate configurations. Field testing of the portable sensing unit has shown that the technique can be conducted in the field with results comparable to the laboratory.

DACCO SCI, INC. believes the sensors will provide the USAF with the necessary information to improve maintenance quality, while decreasing its costs and the number of failures due to corrosion.

INTRODUCTION:

Aircraft structures are susceptible to corrosion caused by moisture augmented by runway or marine salt, exhaust fumes and other atmospheric pollutants, oil/gasoline/diesel fuel spills, and cleaning solvents. The cost of corrosion of aircraft is difficult to determine, but has been estimated at $1-3 billion annually for the USAF alone.[1] In 1990, the per aircraft average annual cost of corrosion maintenance was $185,000.[2] The cost of repairs, maintenance, and replacement is a direct cost. The loss of lives and readiness are additional extremely important indirect costs which cannot be assessed in dollar amounts. According to Hoeppner,[3] corrosion-related accidents resulted in 11 fatalities for the military and 70 fatalities for the civilian air fleet over a recent 17 year period. More recently, the National Transportation Safety Board concluded that undetected corrosion was the cause of a commuter aircraft crash that killed ten people.

Increased effort will be required to maintain adequate safety standards in the face of increased structural deterioration of aircraft with operational lifetimes stretched beyond those expected of aircraft at the time they were built. The age of the USAF fleet is dramatically increasing (Table 1); 2660 Air Force planes, or 57% of the fleet, are over 20 years old.[4] New procurement of aircraft is being reduced or stretched out and these new aircraft will be expected to remain operational for longer times. For example, the C-135 is now expected to remain in service until 2040, at which point, the aircraft will be 70-80 years old.

Table 1. *Average Age and Projected Retirement of Selected Air Force Aircraft.*

	Total	*Average Age (1993)*	*Projected Retirement*
A-10	222	11.2	
B-52	148	31.4	2030
C-5A	77	25	2021
C-9	35	21.5	
KC-10	59	7.7	
C-130	334	21.9	2030
C-135	479	30.9	2040
C-141	241	26.9	2010
F-15	688	8.3	2020
F-16	866	3.7	2020
F-111	232	21.5	
T-37	504	29.8	
T-38	685	26.1	
Total	*4493*	*18.64*	

Modern aerospace systems are designed and constructed of many different materials and must perform efficiently under various climatic conditions. Corrosion problems become very complex in the presence of salt water, engine exhaust fumes, ship stack gases, spillage of fuel oxidizers and hydraulic fluids, torrential rains, and taxiing on runways inundated with salt-containing water. For example, due to the U.S. Air Force's involvement in the desert of the Middle East (Operation

Desert Storm), where airplanes and Combat Systems were subjected to extreme sandblasting, corrosion problems were an immediate concern to the U.S. Military. Sand and other related particulates greatly increased the electrical conductivity of moisture present in and around electrical and electronic equipment and rapidly accelerated corrosion.

Painting is the most common means of protecting a metal structure from corrosion. However, paints or other coatings are only temporary solutions. Paints degrade by moisture absorption, weathering (including attack from ultraviolet radiation and pollutants), abrasion/wear, and other mechanisms.

The goal of this Phase II effort was to develop a corrosion sensor based on our Phase I research using inexpensive electrodes which yield a straightforward indication of the state of aircraft aluminum corrosion under paint coatings. DACCO SCI, INC. believes the sensors will provide the USAF with the necessary information to improve maintenance quality, while decreasing the possibility for failures due to corrosion. This functioning electrode sensor will decrease the service costs of the aircraft in the USAF because it will allow maintenance to be performed on a needs basis when it is relatively inexpensive before damage and loss of capability becomes critical and expensive remedial action is needed. The maintenance schedule would be a proactive one rather than one that reacts to failures.

Two versions of the *in-situ* sensor have been developed: a permanently attached sensor and a portable hand-held sensor. The former is suitable for corrosion inspection in inaccessible areas or for automatic or semi-automatic inspection of a particular area. A laboratory test specimen with an attached sensor is shown in Figure 2. The hand-held sensor is suitable for spot inspection where a permanent sensor is not desired or had not been previously placed. Figure 3 shows a prototype in use.

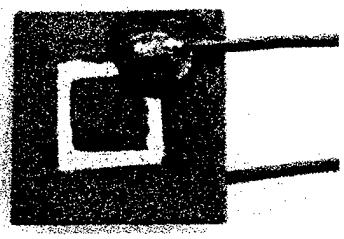

Figure 2. *Painted aluminum test specimen with an attached in-situ corrosion sensor.*

Figure 3. *Hand held in-situ corrosion sensor.*

Electrochemical impedance spectroscopy (EIS) has previously been used to detect coating degradation on steels and other metals in the laboratory.[5-7] Good correlation has been reported between short-term EIS measurements and long-term coating performance during immersion in different electrolytes, demonstrating the technique's predictive capabilities.[8-11] However, these applications involved immersion of the specimen and use of external reference and counter electrodes. Although limited success has been reported on the use of flat cells or similar apparatus for detection of corrosion in the field,[12-14] they require a smooth, flat surface to obtain a seal when using a liquid electrolyte (Table 2). Even the use of gels, sponges, and other solid or semisolid electrolytes can be messy and require access to the location being inspected. Such cells can only detect corrosion directly under the electrolyte.

Table 2. *Comparison of In-Situ Corrosion Probe with Conventional EIS.*

***In-Situ* Corrosion Probe**	**Conventional EIS**
• Suitable for field use or laboratory test chamber/ immersion	• Requires immersion or clamp-on liquid cell
• Permanent electrode is available for inaccessible regions	• Cell requires accessible, flat, horizontal area, messy electrolyte, and remote electrodes
• Hand-held sensor is available for structures/ areas without a permanent sensor	• Set-up is time consuming and must be performed for each measurement
• Arbitrary structure configuration	• Corrosion is detected only directly under cell.
• Easy set-up/inspection	
• Inspection can detect corrosion over large area	

The *in-situ* corrosion sensor offers a quantitative measure of incipient corrosion in the field unlike other corrosion monitors (Table 3). The first field corrosion sensors simply measured the time of wetness of a surface – a useful parameter, but only one factor controlling corrosion. An early *in-situ* sensor provided some of the advantages of the current permanent sensor, but required vacuum deposition of the sensor electrode thus restricting it to small test panels or components.[15-17] Other sensors determine the corrosion rate of the sensor itself using coated optical fibers, mass gain/loss, or electrochemical measurements on witness electrodes that are part

of the sensor package.[18,19] Because of differences in corrosion susceptibility of the witness electrode material(s) and the actual structure and differences in the microenvironment of the sensor and the structure, the corrosion rates measured by the witness sensors may or may not correlate with corrosion rates exhibited by the structure being inspected. Traditional nondestructive evaluation (radiography, ultrasonics, thermography) has required extensive structural degradation – loss of material, blistering delamination of paint, coatings, or of the structure itself. In some cases, these techniques are better suited for detection of strain or cracks (other serious problems) instead of corrosion. As such, they are complementary to the *in-situ* corrosion sensor. Many of these procedures either require sophisticated equipment or highly trained personnel or do not measure the corrosion of the structure of interest. In the case of x-rays, significant safety issues arise with the use of ionizing radiation.

Table 3. *Comparison of In-Situ Corrosion Probe with Other Corrosion Detection Methods.*

***In-Situ* Corrosion Probe**	**Other Corrosion Sensors**
• Measures corrosion of actual structure	• Time of wetness monitors

• Sensitive to early stages of corrosion/degradation	• Corrosion of sensor itself
	  • Material differences
	  • Environmental differences

• Very sensitive to moisture intrusion into bondline	• Require significant loss of material
• Relatively inexpensive instrumentation	• Require delamination or blistering
• Monitors electrochemical process (corrosion) directly	

The *in-situ* corrosion probe is directly applicable to detect the degree of coating degradation and the amount of substrate corrosion of real structures. Because it detects the very early stages of corrosion, it provides a warning before structure degradation occurs. Thus preventative maintenance can be scheduled in time to forestall corrosion damage. Alternatively, by detecting corrosion from the very early stages and allowing a quantifiable comparison between field or service degradation and that observed during accelerated testing, the sensor should be valuable during coating development.

The Phase II program addresses three issues:

- Sensor optimization
- Packaging of instrumentation and electronics
- Establishing the effects of environmental conditions during usage

Sensor optimization included the down-selection of electrode materials that provided the maximum response and the most predictive, reproducible data. Furthermore, the corrosion spectrum for each type of aluminum/coating system was established through accelerated corrosion testing. EIS data from the corrosion testing correlated with ellipsometry and DC electrochemical methods to establish a precise corrosion spectrum for each metal/coating system. The exact range over which the electrode is sensitive was established. Modification of the test instrumentation package involved simplification of the laboratory instrumentation along with the development of analysis software for field use.

Definition of the effect of environmental measurement conditions established the effective electrode range under the limitations of the environment. The limitations of severe environments was addressed in order to develop methods to overcome these limitations.

Background discussions of the following techniques utilized in this research project are provided for:

- Electrochemistry
  - *Electrochemical Impedance Spectroscopy*
  - *Potentiodynamic Testing*
- Ellipsometry

Electrochemistry - Electrochemical Impedance Spectroscopy (EIS)

Analysis of EIS measurements is often based on the fact that the behavior of an electrochemical cell and that of an electronic circuit are analogous. This allows equivalent circuit modeling of a given electrochemical cell. Fundamental AC circuit theory can then be applied to the circuit model and the results accurately correlated to reveal physical and chemical properties of the electrochemical cell.

In an electrochemical cell, the presence of a coating, an electrolyte, and diffusion, act to slow the flow of electrons and each can be modeled as resistors, capacitors, inductors or a combination of elements. These factors give rise to a particular circuit for a given electrochemical cell, such as the one shown in Figure 4.

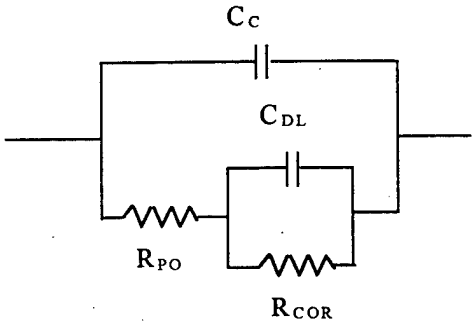

Figure 4. *Equivalent Circuit Model for a Coated Specimen.*

The pore resistance (R_{po}) is the reflection of the amount of penetration by the electrolyte into the coating. The coating capacitance (C_c) is a measure of the effectiveness of the coating. The double layer capacitance C_{dl} and the resistance R_{COR} characterize the coating/metal interface.

Performing conventional EIS on a sample involves applying ac voltage of varying frequencies between a reference electrode and the sample which is immersed in a conductive electrolyte. The current or impedance (magnitude and phase) is measured between the sample and a separate counter electrode. With the DACCO SCI *in-situ* sensor, a single electrode is applied to a coated metal and this electrode acts as both the reference and counter electrodes. Equivalent results are obtained for the two approaches.

Figure 5 shows examples of EIS data, expressed in the Bode magnitude and phase formats, which demonstrates how a typical coated metal degrades in moisture. Initially the coating exhibits purely capacitive behavior (slope of -1 in the magnitude plot and phase angle near 90° in the phase angle plot) with the resistances shown in the equivalent circuit of Figure 4 being very high. As moisture permeates the coating, these resistances decrease and the impedance at low frequencies drops and becomes independent of frequency, corresponding to resistive behavior (phase angle near 0°). As degradation proceeds, the frequency range over which the coating exhibits resistive behavior increases.

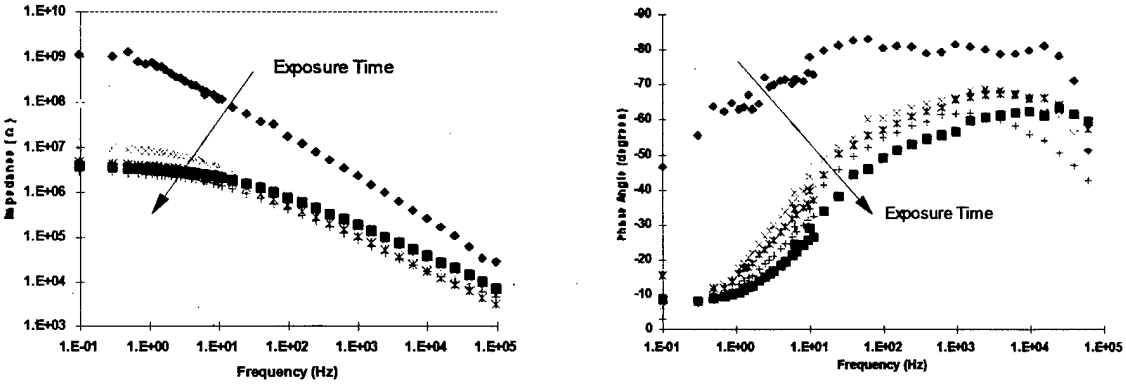

Figure 5. *Bode magnitude(left) and phase (right) plots showing degradation of a coated metal over time.*

Electrochemical Testing - DC Potentiodynamic Scans

DC potentiodynamic scans of a sample provide an indication of the corrosion behavior of the specimen in a test solution environment. A potentiodynamic scan involves sending a current through the specimen and measuring the electrochemical reactions at the interface between the metal and the electrolyte. The corrosion rate of the specimen can be calculated by analyzing the oxidization and reduction reaction rates at the interface. DC corrosion techniques actually induce corrosion in a test sample and provide information on the corrosion rate and the open circuit potential of a given test sample. The DC corrosion technique will aid in verifying the results obtained from EIS by correlating the severity of corrosion with the corrosion rate itself.

DC electrochemical corrosion techniques are used to characterize the overall corrosion behavior of a system. A potentiodynamic scan of a specimen provides information on the open circuit potential and the corrosion rate of a sample in a given electrolyte environment.

The potentiodynamic technique sweeps the potential of a metal specimen slowly over a given potential range. During this sweep, the sample will undergo various electrochemical reactions including oxidation and reduction at the interface of the metal and electrolyte. The rates of these electrochemical reactions are analyzed to yield information on the corrosion potential (E_{corr}), corrosion current, corrosion rate, and mechanistic information.

At potentials less than E_{corr} the sample is considered to be cathodic. This is the region where reduction occurs at the interface and corrosion is not present. At potentials greater than E_{corr} the sample is considered to be anodic. This region is where the sample undergoes oxidation and begins to corrode. At E_{corr} the anodic current is equal to the cathodic current and oxidation occurs as fast as reduction. This is the point where the sample is in equilibrium.

Ellipsometry

Ellipsometry is the measurement of the effect of reflection on the state of polarization of polarized light. Ellipsometry is especially suited for the observation of film formation, integrity, and degradation of metals. The techniques and principles of ellipsometry have been used since the early 1900's. With recent advances in electrochemical testing, the use of ellipsometry has become an increasingly popular tool in the study of corrosion. Furthermore, ellipsometry can be performed simultaneously with electrochemical techniques, such as EIS, to provide another technique for analyzing corrosion.

Ellipsometry reflects light of a known polarization from a substrate (Figure 6). The presence of a film or coating will cause the light to change polarization. This change in polarization is then measured and mathematically correlated with optical constants and film thickness. The use of ellipsometry does not accelerate or alter the integrity or formation of coatings. Therefore, it is an accurate method for verifying electrochemical results.

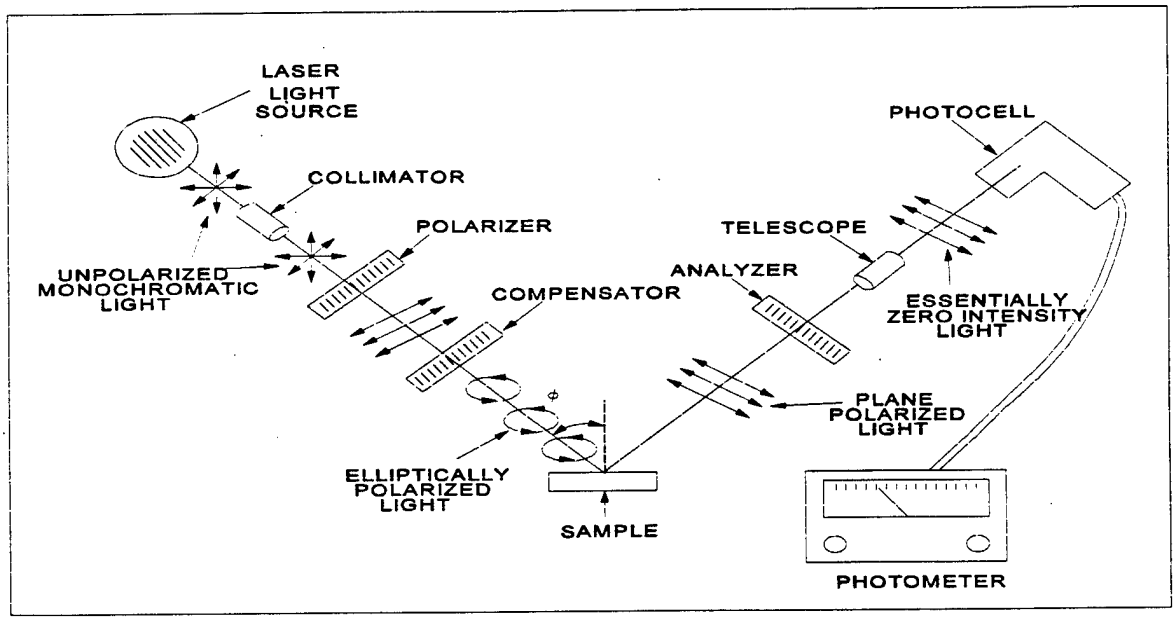

Figure 6. *Components of an Ellipsometer.*

PLAN OF ACTION AND MILESTONES (POAM):

ID	Task Name
1	1. DOWN-SELECT ELECTRODE MATERI/
3	2. ESTABLISH PREDICTABLE BEHAVIOF
5	3. DETERMINE AREA OF COVERAGE
7	4. RESPONSE TO SUBSTRATE CONFIGU
9	5. DESIGN AND FABRICATE FIRST PROT
11	6. FIELD TESTING OF PROTOTYPE
13	7. UPSCALE PROTOTYPE SENSOR DEVI
15	8. TESTING OF UPSCALE SENSOR
17	9. FINAL PROTOTYPE SENSOR DEVELO
19	10. TEST FINAL SENSOR
21	11. INCORPORATE SENSOR INTO AIRCR
23	12. REPORTING

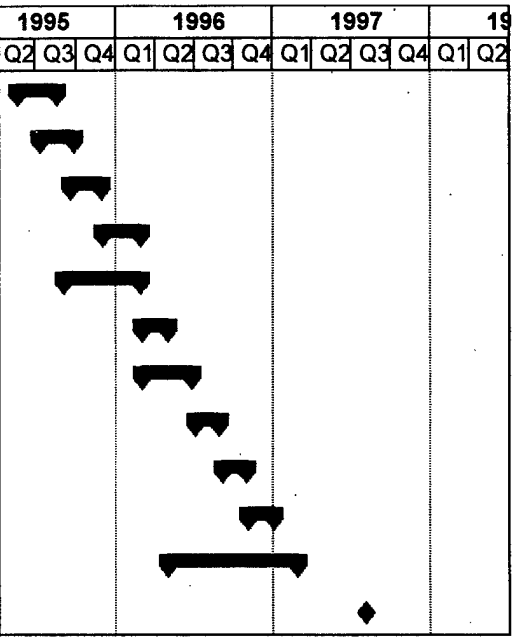

MATERIALS:

1. Sample Preparation for Task 1 (Down-Select) **and Task 2** (Environmental Limitations)

Acquisition and Coating of Aluminum Samples. Sheets of 46" × 46" × 0.032" Al 2024-T3 and Al 6061-T6 were obtained from C-S Metals Service, Inc. A 144" × 48" × 0.032" sheet of Al 7075-T6 was obtained from Davidson Aluminum and Metal Corporation. Each aluminum sheet was machined into seventy-five (75) rectangular samples (1" × 1" × 0.032"). The samples were then sent to Courtaulds Aerospace in Berkeley, CA where they were prepared according to Table 4.

Table 4. *Matrix of Test Samples for Task 1 and 2 Testing.*

Substrate	# of Samples with Waterborne Epoxy (MIL-P-85582) Urethane (MIL-C-85285)	# of Samples with Epoxy Polyamide (MIL-P-23377) Urethane (MIL-C-85285)	# of Samples Left Bare
Al 2024-T3	35	35	5
Al 6061-T6	35	35	5
Al 7075-T6	35	35	5

Application of Interlux to Samples: Interlux is a two-part water resistant epoxy. The Interlux was applied to the edges and backside of the samples to ensure that corrosion would only occur on the front side of each sample, representing the case of an aircraft coating.

Sensor Electrodes: The electrodes were formed by painting a conductive ink grid onto the sample using a small brush. Several conductive inks, epoxy materials, and curing conditions were evaluated. A wire to the ink electrode serves as the reference electrode lead. A wire to the metal backside of the sample serves as the working electrode lead.

Scribing of Samples: Several batches of electrodes were scribed in order to perform accelerated corrosion testing. Scribing was performed according to ASTM D 1654. Two one (1) centimeter lengths inside the electrode area were scribed in the shape of an "X" with the aluminum substrate being exposed.

Control Samples: Several samples were made as control samples. These samples did not have any conductive ink electrode applied and were tested using the conventional three-electrode EIS.

2. Sample Preparation for Task 3 (Area of Coverage)

Al 2024-T3 panels were machined into 12" × 3" × 0.032" and 48" × 6" × 0.032" samples. The samples were sprayed with a household enamel. After the paint cured, Interlux was applied to the edges and back of the sample to provide a water-tight seal. A defect was introduced at one end of the sample by drilling through the coating.

3. Sample Preparation for Task 4 (Response to Substrate Configuration)

Al 2024-T3 panels were machined into 6" × 6" × 0.125" samples. Al 7075-T6 samples were machined into 6" × 1" × 0.032" samples. Three different lap joint configurations were assembled. Lap joint #1 was constructed using rivets only (Figure 7). Lap joint #2 used a modified epoxy adhesive by Cytec to join the parts. Lap joint #3 used both adhesive and rivets. After assembly, each sample received three coats of bare metal primer and two coats of an enamel topcoat. After the paint cured, Interlux was applied to the edges of each sample.

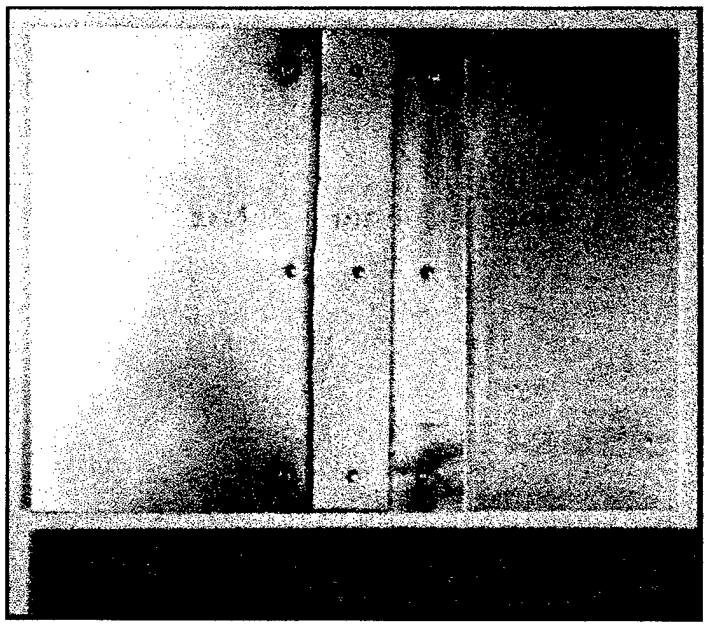

Figure 7. *Lap Joint Configuration (Rivets).*

4. Sample Preparation for Task 6 (Field Testing of Prototype Sensor)

Three (3) 6" × 6" × 0.125" panels and two (2) 1" × 6" × 0.125" panels of Al 2024-T3 were used to field test the prototype hand-held corrosion sensor. The panels were painted with two coats of bare metal primer and four coats of a spray enamel. Prior to testing each panel was holiday tested using a low voltage Tinker & Rasor holiday detector to ensure a defect-free coating. The edges and the region around the wire connection were then coated with Interlux.

TESTING PROCEDURE:

Laboratory EIS Technique

Laboratory EIS was performed using the EG&G Princeton Applied Research (PAR) Potentiostat Model 273. An EG&G PAR Lock-in Amplifier Model 5210 was used to generate the alternating current waveform. EG&G PAR Model 398 version 1.10 Electrochemical Impedance software was used.

The EG&G PAR K0235 Flat Cell electrochemical cell was used for the conventional three-electrode EIS measurements. A 0.05 M Sodium Sulfate (Na_2SO_4) solution was used as the electrolyte. The corrosion cell requires the use of a reference and counter electrodes.

Testing of samples with the conductive ink electrodes or the prototype sensors was done without the use of an electrochemical corrosion cell. The working electrode was connected to the metal backside of the sample. The reference and counter electrodes were electrically connected to the sensor electrode lead.

Field EIS Technique

Field EIS was performed using the Gamry Instruments CMS 100 Corrosion Measurement System in conjunction with the Gamry Instruments CMS 300 Electrochemical Impedance System software. The Gamry CMS system was installed in a portable computer. The connections for three-electrode and two-electrode EIS remain the same as for the EG&G unit.

DC Potentiodynamic Scans

The EG&G PAR Potentiostat Model 273 with the EG&G PAR Model K47 Corrosion Cell was used to perform potentiodynamic scans according to ASTM G5 on the samples to calculate instantaneous corrosion rates. A 0.05 M Na_2SO_4 solution was used as the electrolyte. The sample was then immersed completely in the electrolyte and electrically connected as the working electrode. A reference electrode was positioned next to the sample and connected to the potentiostat. Two graphite rods immersed in the electrolyte acted as the counter electrodes. Using the EG&G PAR Model 352 SoftCorr II Corrosion Measurement and Analysis Software, DC current was then sent through the sample and the corresponding corrosion potential was measured versus the corrosion current. The instantaneous corrosion rate and protection potential were then calculated from the resulting data. The testing procedure was identical for the control samples and the samples with the sensor electrodes.

Ellipsometry

Ellipsometry was conducted using the Gaertner Scientific Model L119x Ellipsometer using a 4 mW Helium-Neon laser with a wavelength of 6238 Å. Gaertner Scientific GS-SC4A L104 software package was used to automatically control the photocell and determine the null point.

The index of refraction, coefficient of extinction, ψ, and Δ were then calculated. Multiple measurements were taken for each sample to obtain more precise results.

Salt Fog Testing

Salt spray testing was conducted using the Singleton Corporation SCCH Corrosion Test Cabinet Model 20. A 5% Sodium Chloride (NaCl) solution at 99°F was used. Salt fog testing was conducted according to ASTM B117. Testing was interrupted only when EIS tests on the samples were scheduled. When removed from the salt fog chamber, each sample was rinsed with distilled water, dried with a nitrogen stream, and measured within twenty (20) minutes or less of removal.

Temperature/Humidity Testing

Humidity testing was conducted using the Blue-M Environmental Chamber Model #VP-100AT-1. The operating temperature and humidity ranges of the chamber are 25°C to 90°C and 25% RH to 99% RH, respectively. The chamber allowed for *in-situ* EIS measurements with the conductive electrode sensors and chamber feedthroughs.

Testing at temperatures below 25°C were conducted in a Sanyo Refrigeration Unit.

RESULTS AND DISCUSSION:

The purpose of the Phase II research was to develop a corrosion sensor that is capable of detecting corrosion on aircraft at early stages. Phase I research accomplishments were:

- Proving the feasibility of using Electrochemical Impedance Spectroscopy (EIS) to evaluate coating performance
- Showing that EIS could detect hidden corrosion at early stages
- Developing both permanent and hand-held *in-situ* corrosion sensors that were capable of utilizing EIS to evaluate coatings and detect corrosion using a two-electrode approach that did not require an electrolyte

TASK 1: Establishing Degradation Behavior of Aircraft Coatings & Down-Selecting Electrode Materials.

Samples were fabricated using Al 2024-T3, Al 6061-T6, and Al 7075-T6 coated with aircraft paint schemes according to military specifications. The combination of the three aluminum substrates and two coating schemes yielded a total of six metal/coating systems that were tested and evaluated.

Electrode sensor grids were placed on some of the samples using different conductive inks. These conductive ink grids were bonded directly to the coating enabling two-electrode EIS measurements without the need for an electrolyte. Phase I results showed that our attached *in-situ* sensors generated impedance data equivalent to the conventional three-electrode approach with electrolyte.

Accelerated corrosion testing using salt fog (ASTM B117) and immersion testing (ASTM D870) was performed on the six metal/coating system samples with and without the sensor electrodes to establish how the coatings degraded electrochemically and to see if our electrode sensors were capable of evaluating a degrading coating.

Samples tested in the salt fog chamber were periodically removed and tested using the three-electrode method. To characterize the degradation behavior of the samples, the impedance in the low-frequency regime (1 Hz) was plotted versus the exposure time. It was found that both the aircraft coatings were resistant to corrosion and showed no indication of actively corroding after seventy-five (75) days of exposure. Samples with an intentional defect were also tested in the salt fog chamber to characterize the electrochemical behavior of the corroding sample. Figure 8 shows the corrosion curves for Al 6061-T6 samples with and without defects for both coating systems. Samples with the epoxy polyamide primer and waterborne epoxy primer are labeled as *EP* and *WB*, respectively. Similar results were obtained for Al 2024-T3 and Al 7075-T6.

The data indicate that the mil-spec coatings are very effective in resisting corrosion. The samples without an intentional defect showed no signs of active corrosion even after 75 days in a 100°F, 98% RH environment. Both coatings exhibited a sharp drop in impedance within the first few

days of exposure indicating a short water uptake stage. However, the waterborne epoxy primer appears to absorb more water during this stage, as seen by the lower impedance than the epoxy polyamide primer, indicating that the epoxy polyamide primer is more effective in resisting water absorption.

The impedance of the epoxy polyamide primer during the incubation stage was typically higher than that of the waterborne epoxy primer. The degree of difference between the coating systems varied from about half an order of magnitude for Al 7075-T6 to one and a half orders of magnitude for Al 6061-T6. In addition, the impedance of the epoxy polyamide primer was typically slightly higher in the active corrosion region.

Based on these plots, a single low frequency impedance measurement can be made on a coating to characterize the stage and severity of corrosion that the coating is experiencing. Once the low-frequency impedance reading has been measured, the corresponding impedance can be found on the corrosion behavior curve for the appropriate metal/coating system.

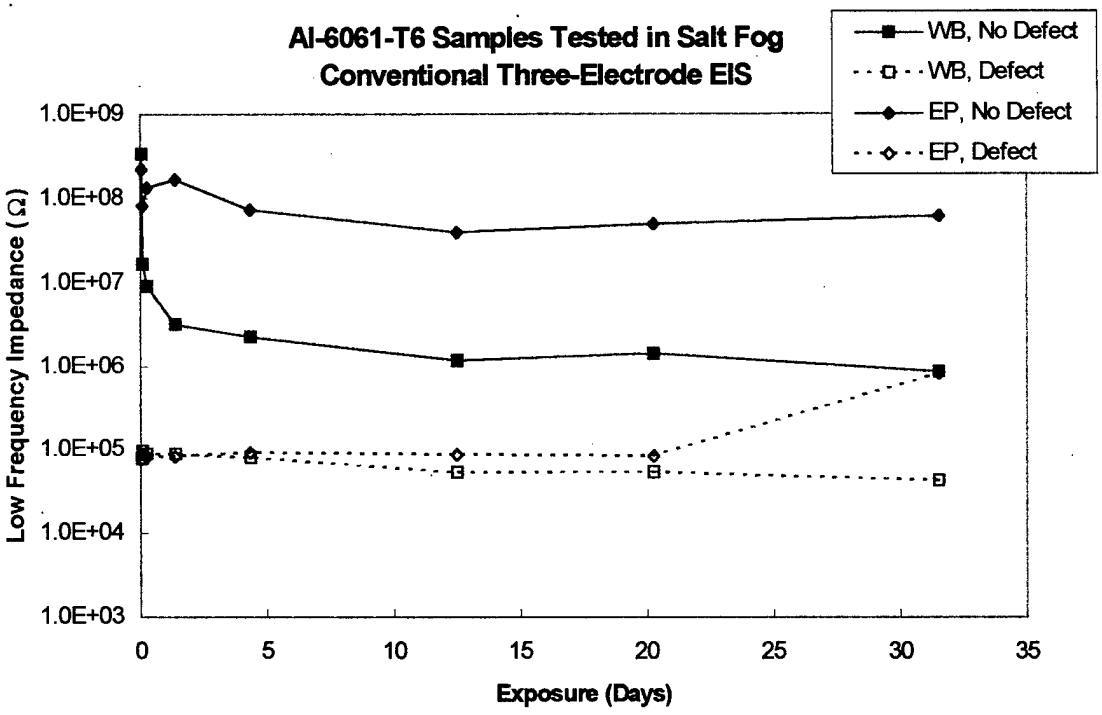

Figure 8. *Corrosion Behavior of Coated Al 6061-T6 Tested in Salt Fog.*

Immersion Testing

Immersion testing was conducted on samples that were scribed with an intentional defect in the center in the shape of an "X". Samples were immersed in 5% NaCl solution and removed only to perform testing. The purpose of the testing was to determine whether changes in the low-frequency impedance of the coating can be correlated with changes in the corrosion rates and refractive index. Testing of the samples included:

- EIS to ascertain coating impedance
- Ellipsometric testing to characterize the refractive index
- Potentiodynamic testing to determine corrosion rates

Low Frequency Impedance

The impedance data collected for the Al 2024-T3 samples with epoxy polyamide primer and waterborne epoxy primer are displayed in Figure 9.

The relative times and impedance decreases for the different stages will depend on the quality and chemistry of the coating, the metal underneath and any surface treatment, and the exposure conditions. For example, Figure 9 demonstrates that a waterborne coating is not as effective as an epoxy polyimide coating even with both of them having an urethane topcoat. The impedance of the waterborne coaitng drops approximately one order of magnitude more than the organic solvent coating, reflecting the greater moisture uptake. Partially as a result of the increased moisture concentration at the interface, the incubation period is shorter and active corrosion of the substrate occurs sooner. In addition, since these samples already contained a defect, the low frequency impedance values reflect only very short durations of water uptake.

Refractive Index

The data collected using the ellipsometer were fairly consistent from sample to sample for the individual metal/coating systems. It appeared that the coating was not a significant factor in the measurement of the refractive index of the aluminum substrate, as similar results were obtained for each coating. All of the samples initially exhibited a sharp drop in the refractive index within the first 15 days of immersion. This sharp drop demonstrates that the reflected light off the substrate is not being dispersed significantly, indicating that the aluminum substrates are resisting corrosion and not exhibiting heavy oxide growth. This correlated well with visual observations, during which no significant changes were observed in the luster of the aluminum surface. Figure 10 shows the refractive index of the samples coated with epoxy polyamide primer.

The Al 2024-T3 and Al 6061-T6 samples appeared to behave in a similar fashion. After the initial drop in impedance after 15 days, the refractive index leveled out and then slightly increased by the end of the 50 days testing period. These aluminum substrates had a slight discoloration and loss of luster by the end of the testing. The Al 7075-T6 samples exhibited a sharp increase in the refractive index after 15 days indicating an increase in the rate of corrosion. This was confirmed visually by a significant discoloration of the aluminum and a loss of luster. Corrosion products

were forming at a much greater rate than on the Al 2024-T3 and Al 6061-T6 samples. This rapid increase in the refractive index indicated greater dispersion of light due the more intense formation of corrosion products. After 30 days of immersion, the corrosion products on the substrate dispersed the light enough so that subsequent measurements could not be taken.

Potentiodynamic Testing

The values for the instantaneous corrosion rates obtained from analysis of the potentiodynamic data had significant deviation from sample to sample. The coating system did not appear to influence the measured corrosion rate of the samples. Corrosion rate data correlated well with the ellipsometry data. Initially, all the samples displayed extremely low instantaneous corrosion rates, which is expected for aluminum. After about five days of immersion, the samples typically had a significant increase in the instantaneous corrosion rate. Al 2024-T3 and Al 6061-T6 had similar corrosion rates throughout the testing, while Al 7075-T6 exhibited a sharper increase in corrosion rate, characteristic of its lower corrosion resistance. Corrosion rate data are shown in Figure 11.

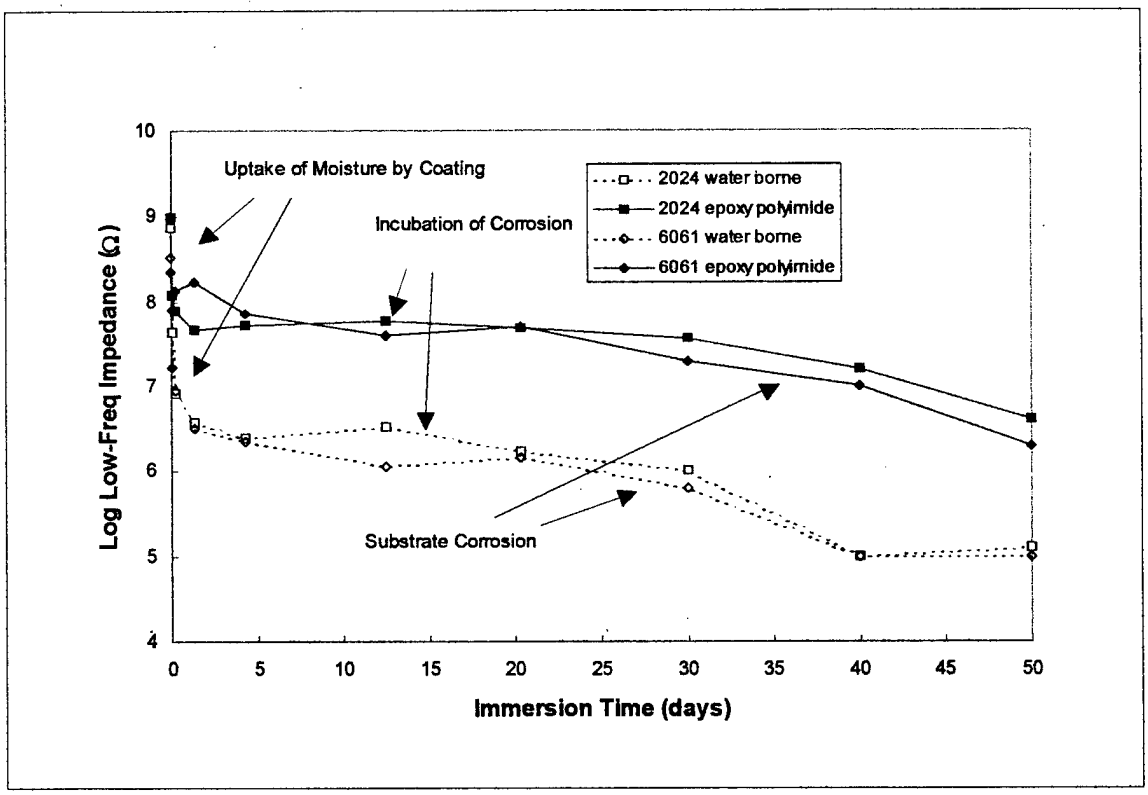

Figure 9. *Corrosion Behavior of Immersion Tested Al 2024-T3 Samples.*

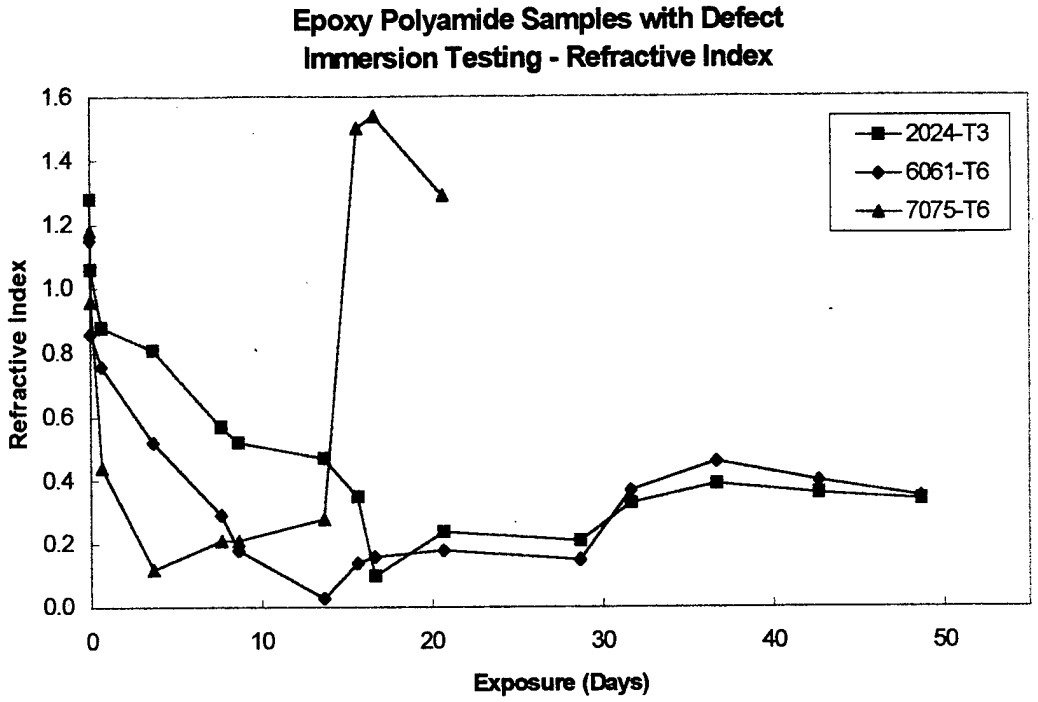

Figure 10. *Refractive Index of Immersion Tested Al samples with Epoxy Polyamide.*

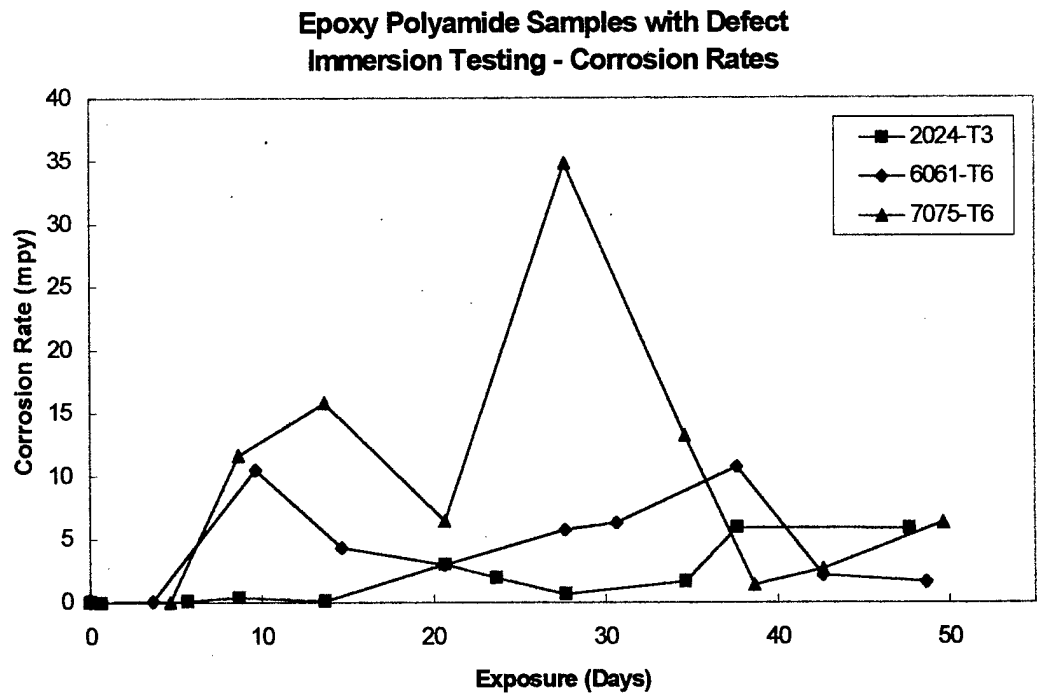

Figure 11. *Corrosion Rates of Immersion Tested Al samples with Epoxy Polyamide.*

TASK 2: Establishing Predictable Electrochemical Impedance Spectra for the Sensor Reference Electrode Versus the Aluminum Substrate.

Testing of the attached *in-situ* electrodes during Phase I and Task 1 was conducted at room temperature and humidity (approximately 25°C and 30% RH). At these ambient conditions there has been no difficulty in acquiring data that are equivalent to the three-electrode method. In Task 2, testing was conducted at a variety of extreme environmental conditions in order to determine if the attached *in-situ* sensors had difficulty in acquiring data and to verify the accuracy of the data. Testing was conducted in an environmental chamber where the conditions could be closely monitored. The EIS measurements using the nickel ink electrodes could be made in-situ during exposure to environmental conditions.

The instrumented samples and control samples (samples without electrodes) were first tested at 40°C and 70% RH. These samples were fabricated from Al 2024-T3 coated with waterborne epoxy primer. Low frequency impedance results are displayed in Figure 12. In-situ testing of the ink electrode sensors revealed there was no difficulty in acquiring data. Furthermore, data accuracy was confirmed by comparing the samples to the control samples which were tested using the three-electrode method.

Testing was then conducted at 40°C and 98% RH on Al 6061-T6 samples coated with epoxy polyamide and waterborne epoxy primer (Figure 13). The elevated humidity increased the rate of initial water absorption as seen by the sharp drop in low-frequency impedance within the first thirty minutes of exposure in the environmental chamber. Samples with the waterborne epoxy primer exhibited a sharper drop in impedance during the environmental testing than the samples with the epoxy polyamide. This behavior was also witnessed in Task 1 testing.

Testing was then conducted at 0°C and 20% RH on Al 2024-T3 samples coated with waterborne epoxy primer (Figure 14). There was no difficulty in acquiring the data, however, the low-frequency impedance data did not yield as smooth a plateau. Some deviation was seen in the impedance values of the low-frequency regime, but an evaluation of the coating could still be easily made based on the data.

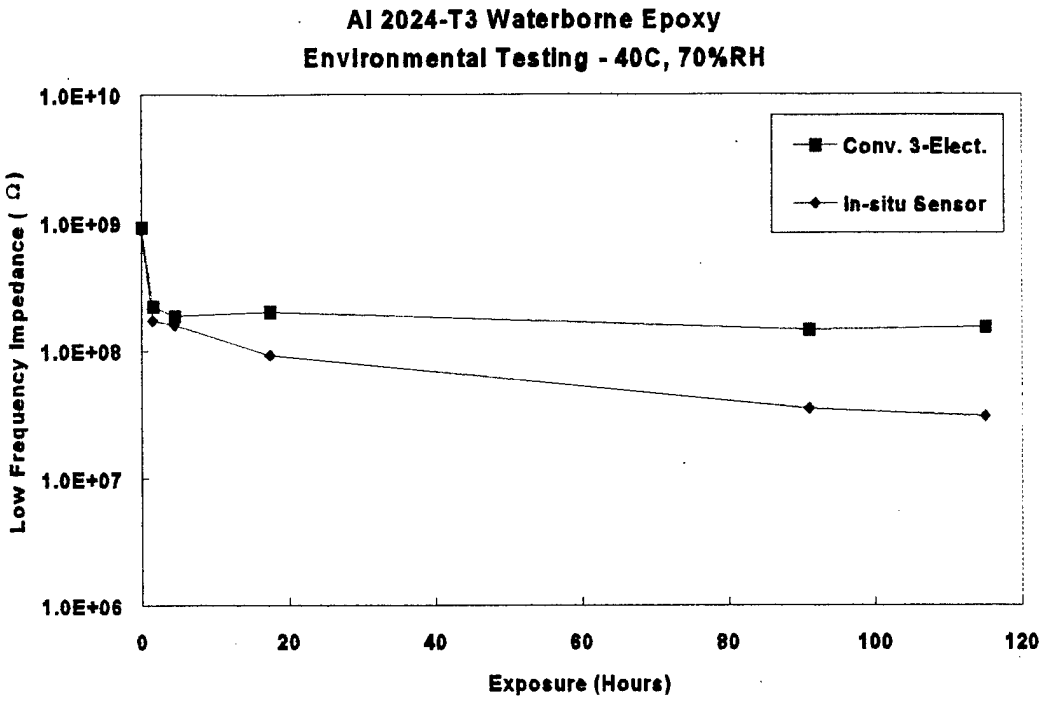

Figure 12. *Corrosion Behavior of Al 2024-T3 with Waterborne Epoxy at 40 °C, 70% RH.*

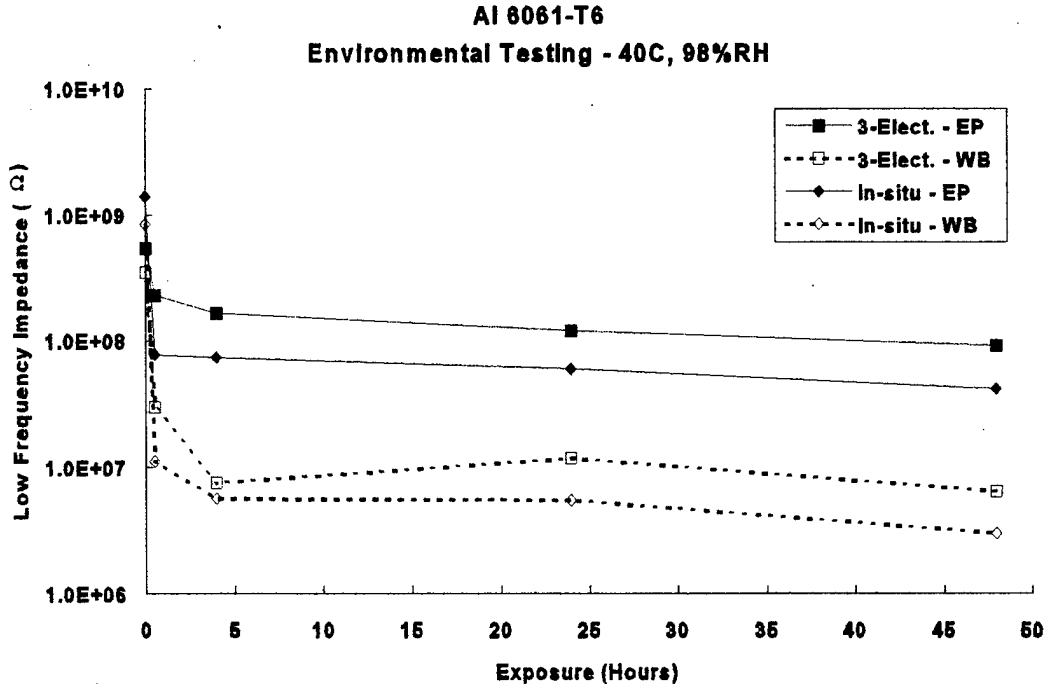

Figure 13. *Corrosion Behavior of Al 6061-T6 Samples at 40 °C, 98% RH.*

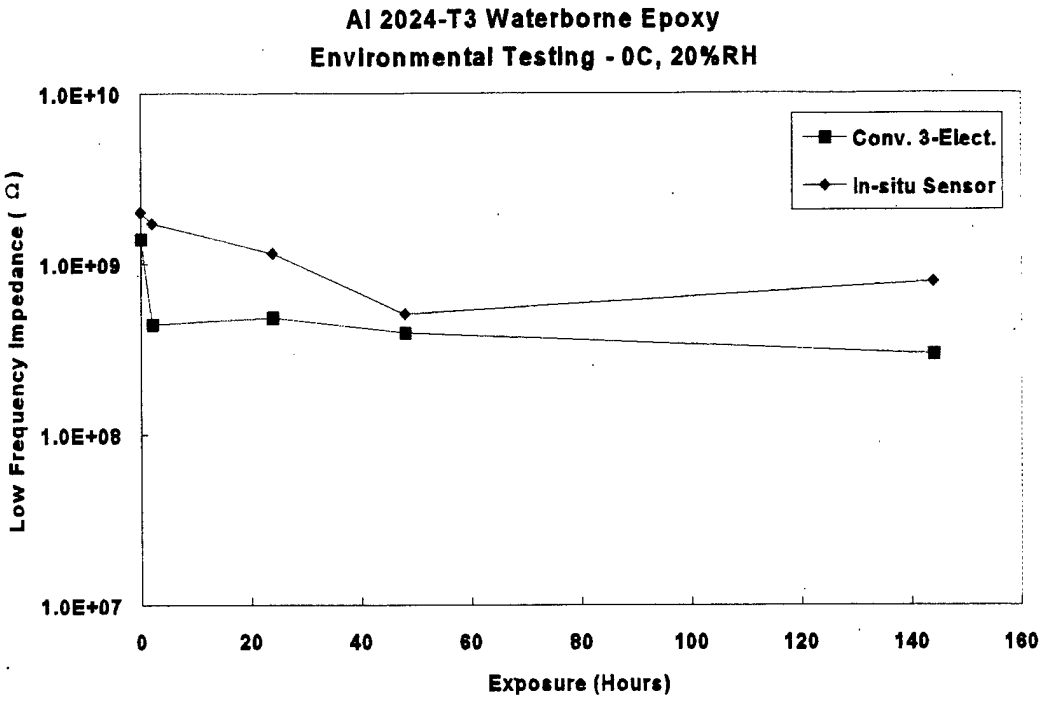

Figure 14. *Corrosion Behavior of Al 2024-T3 with Waterborne Epoxy at 0 °C, 20% RH.*

TASK 3: Determination of the Area of Coverage for the Prototype Electrode.

Task 3 was conducted using the first set of prototype electrodes (See Task 5 and 6 results). Testing was performed in order to determine the effective range that the sensors could detect coating degradation. Initial testing indicated that the sensors could only detect coating degradation underneath the sensor itself on a dry surface. On a wetted surface, though, the effective range of the sensor is appreciably increased. In the laboratory, a conductive path was created artificially through the application of a couplant. In the field, the paint surfaces could be wetted to provide surface conductivity. Figure 15 shows the effect of the presence of a couplant on the impedance spectra of Al 2024-T3 coated with epoxy polyamide primer before and after an intentional defect.

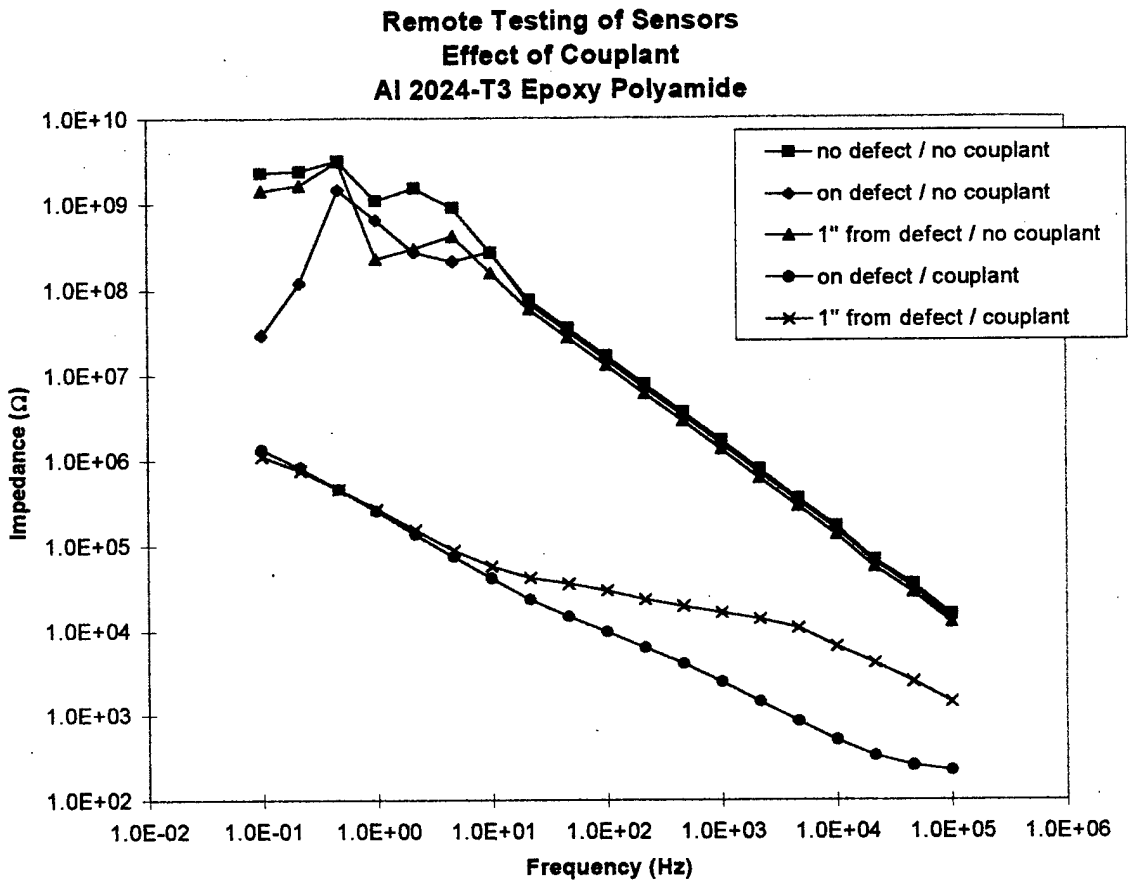

Figure 15. *Effect of Couplant on Impedance Spectra of Defective Coating.*

A variety of couplants, including tap water, isopropyl alcohol (IPA), 0.05 M Na_2SO_4, and an ultrasonic couplant (Exosen 30 by Krautkramer Branson) were tested on 3" × 12" panels fabricated from Al 2024-T3 coated with a spray enamel. Electrical conductivities of each of the couplants are listed in Table 5 below.

Table 5. *Conductivities of Couplants used in Area of Coverage Testing.*

Couplant	Conductivity (μmhos)
Tap Water	189.4
Isopropyl Alcohol (IPA)	0.3
0.05 M Na_2SO_4	8260
Exosen (Ultrasonic Couplant)	1824

The results of the testing using the different couplants indicate that all of them enable the sensor to detect a defect in the coating even at lengths of 12" away from the defect, provided that there

is an uninterrupted path between the sensor and the defect with the couplant. IPA has a low electrical conductivity and thus, as the distance from the defect increases, the low frequency impedance experiences a significant increase. This fact, along with its low viscosity, make it an unattractive couplant alternative for use with the sensor. The response with water and Na_2SO_4 are acceptable for identifying defects, however, their low viscosity may hinder field applications. The ultrasonic couplant provided both the best response to increased distance from the defect and highest viscosity, allowing for use on sloped surfaces.

The next set of tests were conducted to determine the effective range of the sensor using exosen as a couplant. For this testing a 48" × 6" × 1/32" Al 2024-T3 panel coated with a spray enamel was used. Before the defect was introduced, a series of baseline tests were conducted to measure the impedance of the proposed defect location from distances up to 46". After the defect was created, the results show that it could be identified up to 46" away. However, the difference in impedance between the defective and non-defective coatings became increasingly small due to the resistance of the couplant. Under carefully controlled laboratory conditions, a defect was identified at distances up to 180" from the defect site (Figure 16). Figure 17 shows a plot of the plateau frequency (i.e., where the slope of the impedance spectra is zero) impedance versus distance from the defect. A nearly linear relationship exists between the plateau frequency and the distance from the defect.

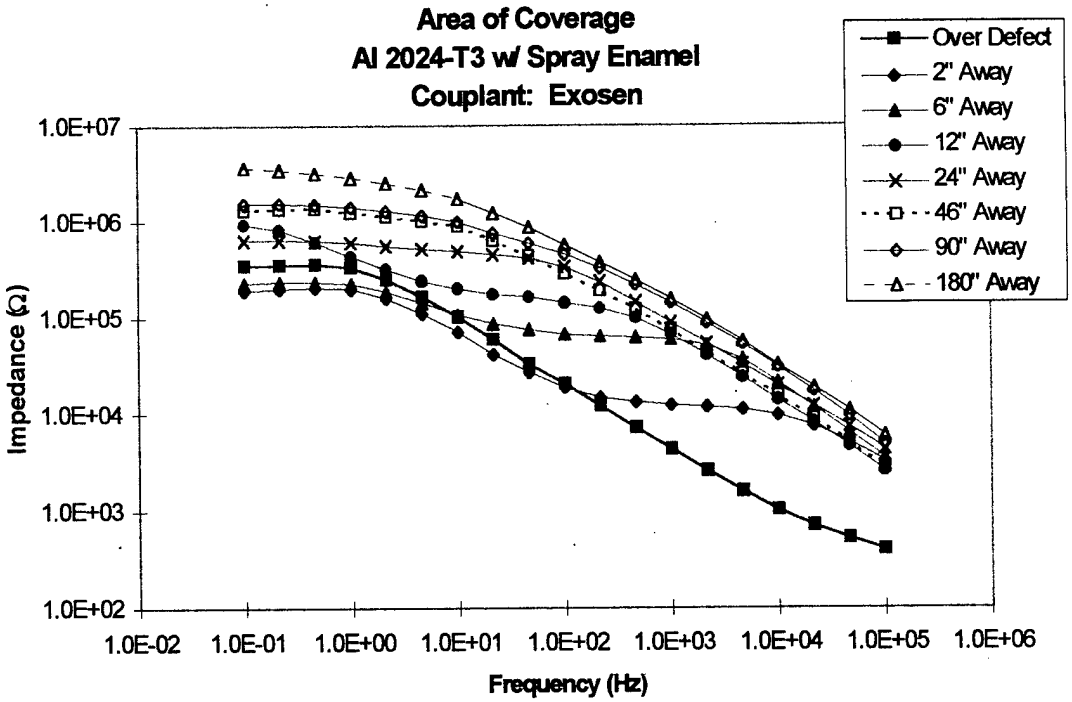

Figure 16. *Area of Coverage Testing with Beaded Couplant.*

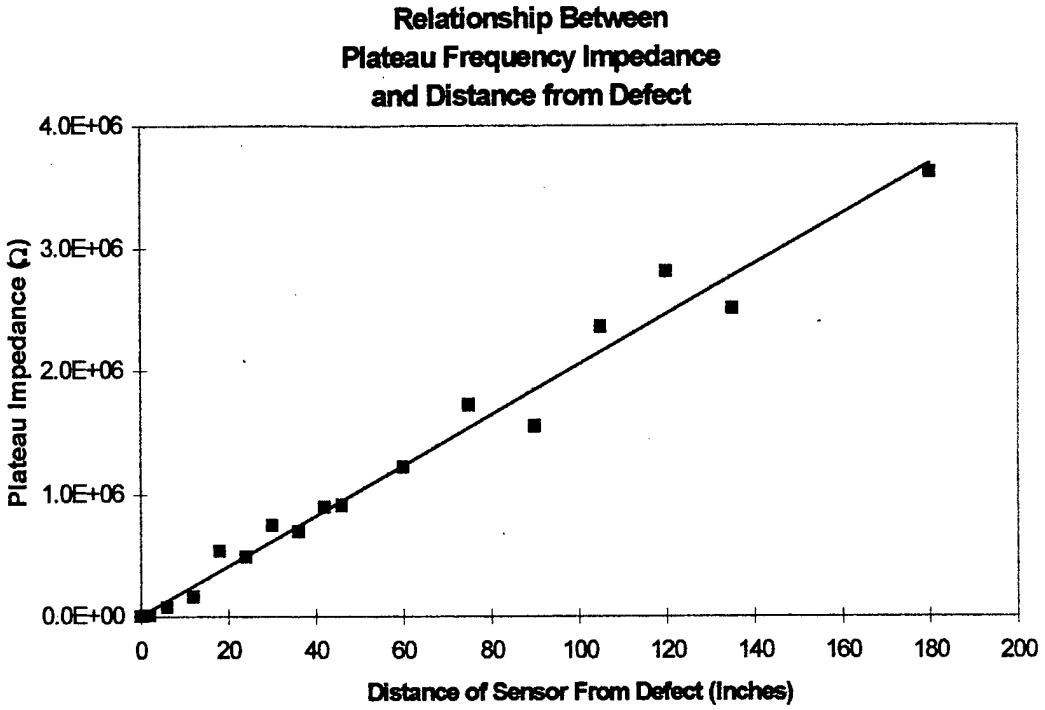

Figure 17. *Relationship Between Plateau Frequency Impedance and Distance from Defect.*

Task 4. Determination of Electrode Response to Various Substrate Configurations.

In Task 4 various aircraft skin configurations were examined. The testing in the previous tasks represents skin and rib configurations. The sensors have proven to work well on these surfaces. The analysis in Task 4 was limited to an investigation of the use of the sensor on lap joint configurations. Three lap joints were tested:

- Lap Joint #1 (LJ1) - Rivets only
- Lap Joint #2 (LJ2) - Adhesive only
- Lap Joint #3 (LJ3) - Rivets and adhesive

Each lap joint has three panels. Panels 1 and 3 are the Al 2024-T3 top and bottom panels, respectively. Panel 2 is the Al 7075-T6 rib on the bottom of the lap joint.

LJ1 and LJ3 responded in similar fashion since each of their three components were made electrically continuous by the rivets. The results indicate that a defect on panel 1 could be identified from panel 1 or panel 3 regardless of the location of the working electrode connection. Measurements were made diagonally from the defect to the opposite corner of the lap joint. Figure 20 shows the impedance spectra of LJ1with the working electrode (WE) connection to Panel 1 (P1) and Panel 2 (P2). The measurement taken 6" from the defect is on Panel 1, while the 10" measurement is on Panel 3. Exosen was used as a couplant.

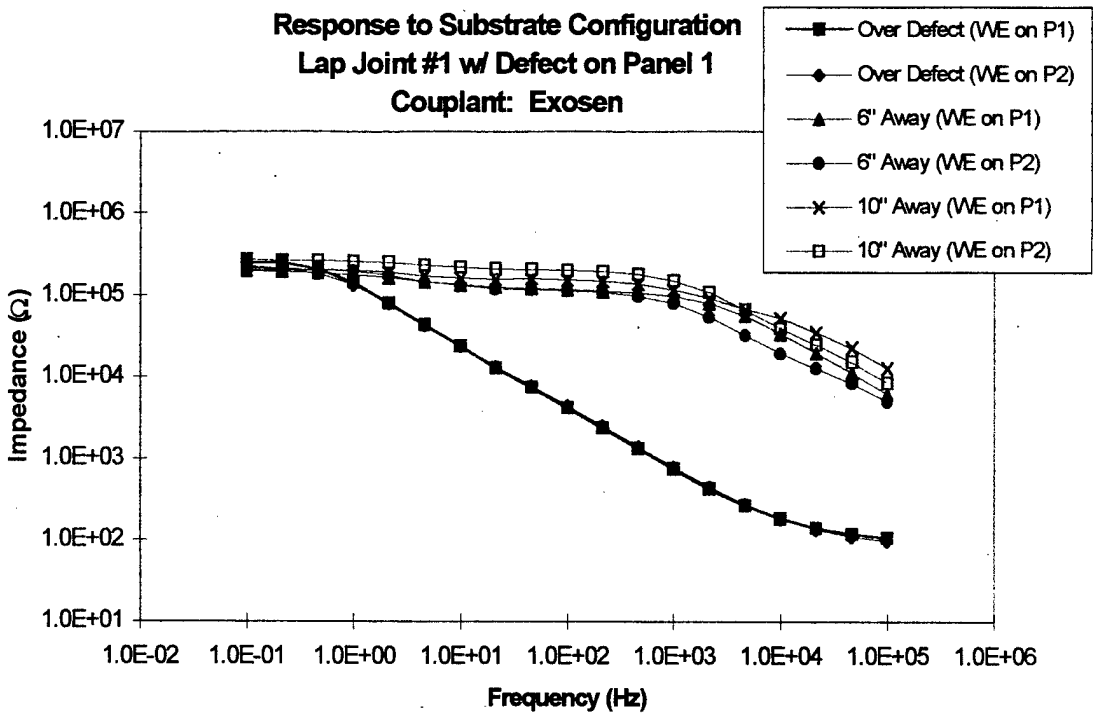

Figure 18. *Impedance Spectra of Lap Joint #1.*

Lap Joint #2 was constructed using adhesive only. As a result, each panel was electrically isolated from the other. If the working electrode is placed on a panel adjacent to the panel with the defect, the impedance measurements will reflect resistance contributions from the coating and the adhesive. Since the impedance of the adhesive is typically very high, a defect in the coating can be difficult to detect. However, it is possible to inspect both the coating and the adhesive with the reference sensor. Figure 19 shows the impedance spectra of a defective coating as measured from the same panel as the defect and across the joint from the defect. The difference in the spectra represents the impedance of the adhesive.

Potentiodynamic testing, including cyclic polarization scans, was conducted on Al 2024-T3 and Al 7075-T6 to determine whether the lap joint configuration was susceptible to crevice and galvanic corrosion. Testing was conducted in 5% NaCl. Results of the testing show that the likelihood of pitting and crevice corrosion are low due to a small hysteresis loop. Galvanic corrosion is also unlikely due to the similar open circuit potentials. One concern for galvanic corrosion is in the choice of rivets. Dissimilar rivet metals may create a galvanic cell with the substrate aluminum which could cause the metal around the rivet or the rivet itself to corrode and result in failure of the lap joint.

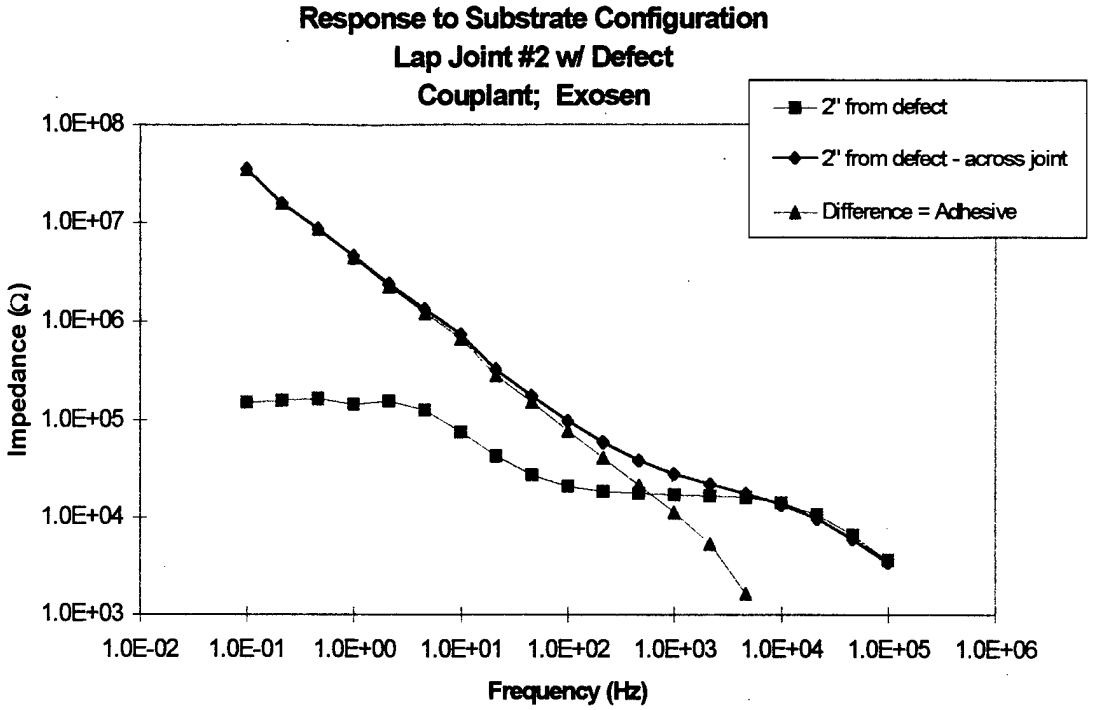

Figure 19. *Impedance Spectra of Lap Joint #2.*

Task 5. Design and fabrication of the first prototype hand-held sensor.

The first prototype electrodes were fabricated from a piece of Al 2024-T3 cut into various shapes and sizes. A lead wire was bonded to the surface of the Al 2024. Baseline testing showed that the prototype electrodes obtained data equivalent to the three-electrode method for samples with and without defects. Figures 20 and 21 show a comparison of the impedance spectra obtained from the three-electrode method and the prototype sensor for Al 7075-T6 coated with epoxy polyamide and waterborne epoxy primers, respectively.

These prototype electrodes were used to acquire the data for Tasks 3, 4, and 6.

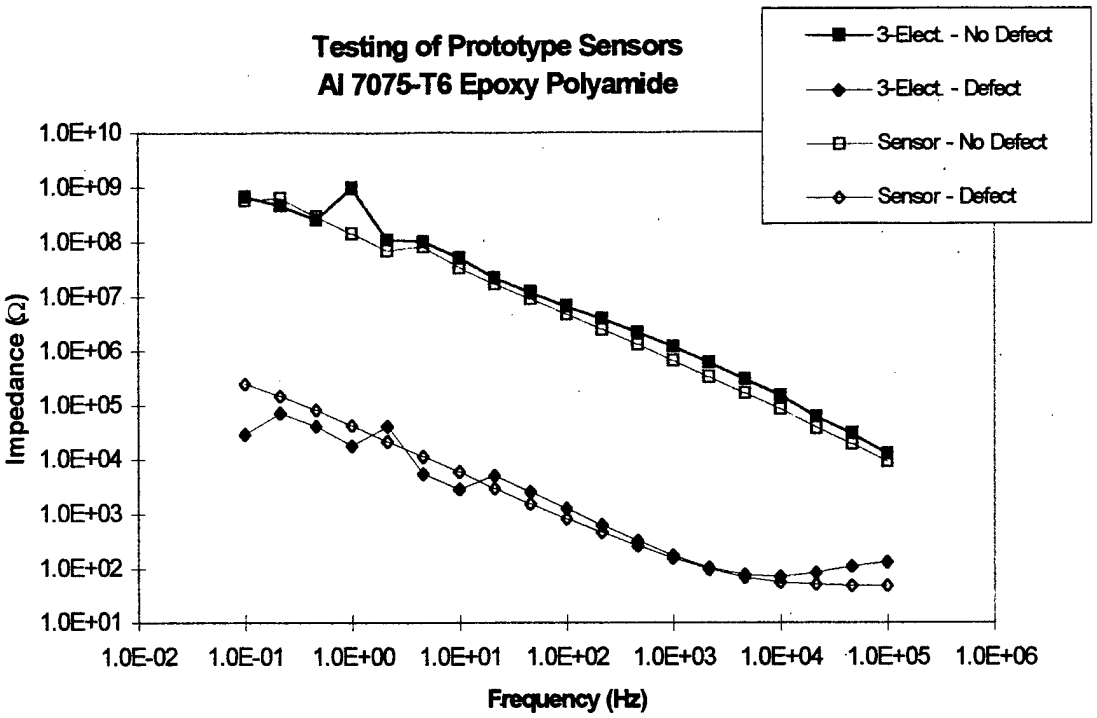

Figure 20. *Impedance Spectra of Al 7075-T6 with Epoxy Polyamide.*

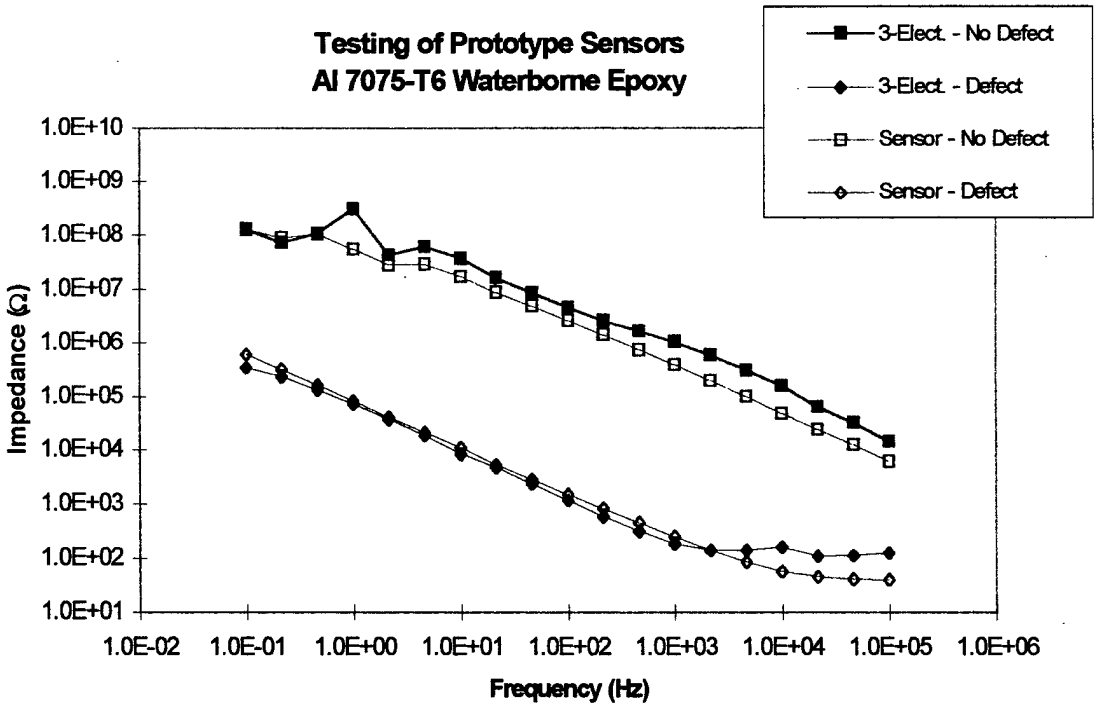

Figure 21. *Impedance Spectra of Al 7075-T6 with Waterborne Epoxy.*

Task 6. Field Testing of the Prototype Sensor.

In Task 6, the prototype sensor was tested in a field environment using the Gamry Instruments portable unit. Before field testing began, several laboratory tests were conducted to fine tune the performance of the prototype sensor leading to the development of the upscale hand-held sensor.

First, extensive analysis was conducted to establish that the Gamry unit was capable of obtaining results equivalent to the EG&G setup. Figure 22 shows the impedance spectra of Al 6061-T6 with waterborne epoxy coating as measured by both the Gamry and the EG&G units using two-electrode EIS. The plot shows that the two systems yield remarkably comparable results. Similar overlays were obtained for the other metal/coating systems.

Laboratory testing was also conducted to determine if the amount of pressure applied to the sensor affected the results of the impedance spectra. Experiments were conducted using both the EG&G and Gamry potentiostats to establish whether either system was sensitive to the pressure on the sensor. Three different ranges of pressure were tested:

1. no pressure (sensor set on bead of exosen)
2. "mild" pressure (200 gram weight on sensor)
3. "heavy" pressure (2000 gram weight on sensor)

The results in Figure 23 show that consistent results were obtained on both systems with all of the test pressures. This is an important finding because field testing with the upscale sensor requires hands-on use. It is believed that the force required to keep the sensor on the testing surface will be adequate to yield consistent results.

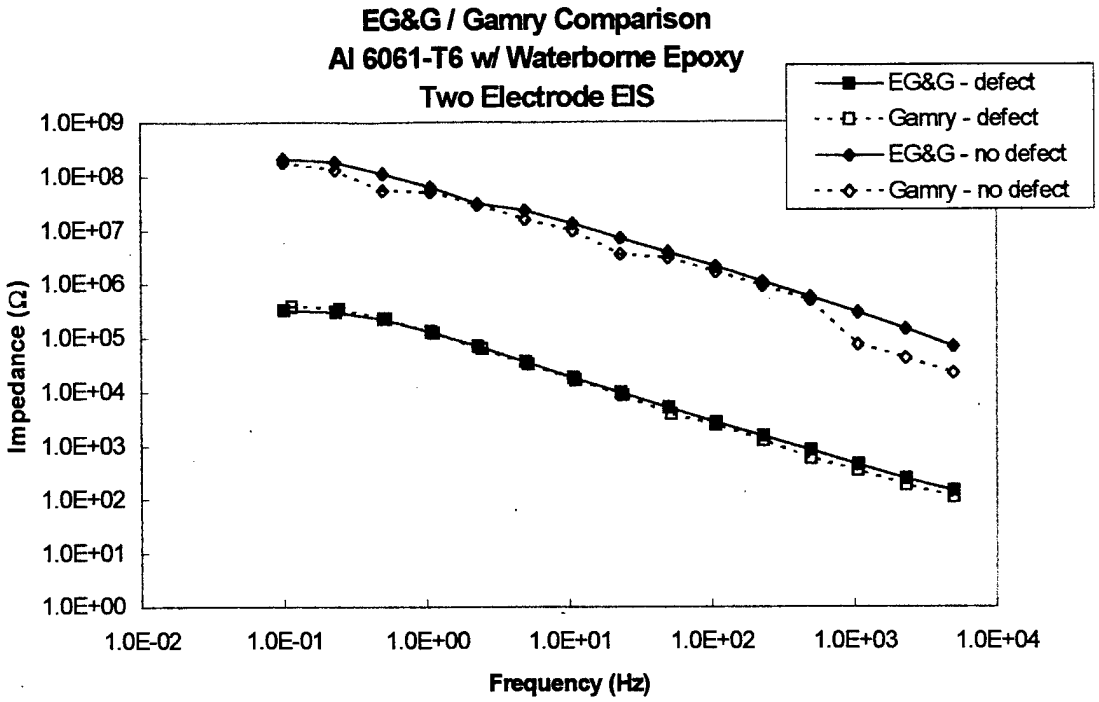

Figure 22. *Comparison of EIS Data Acquired by EG&G and Gamry Units.*

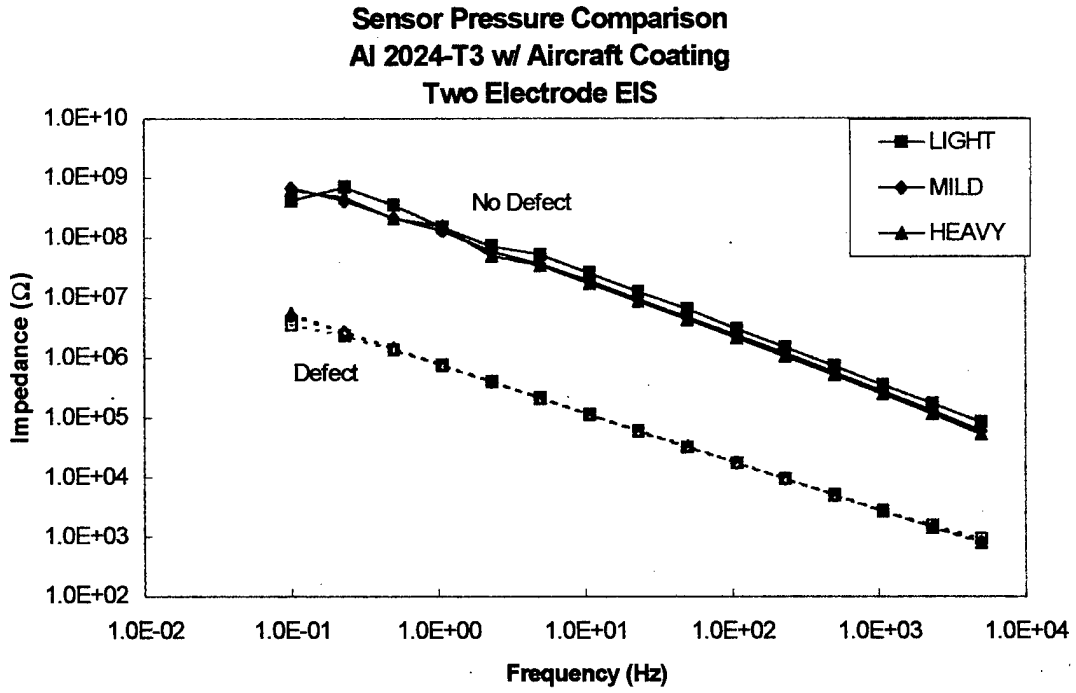

Figure 23. *Effect of Pressure Applied to Sensor on Impedance Spectra.*

Five Al 2024-T3 panels coated with spray enamel were used for field testing. Two 6" × 6" panels (Panels #1 and #2) were secured to a fence along a highway so that they could be exposed to environmental weathering, automobile exhaust, and salt spray from de-icing compounds. Baseline testing of the coatings was completed in the laboratory before field exposure. The panels were tested in the field using the upscale prototype sensor (See Task 7 and 8). The low frequency impedance results show that, for this coating system, the water uptake process is reversible. Decreases in the low frequency impedance were observed after periods of precipitation, usually followed by a return to baseline impedances following a drying out period (Figure 24).

One coated 6" × 6" panel (Panel #3) was maintained at ambient conditions in the laboratory to serve as a control. The low-frequency impedance spectra for this panel shows that very little drop in impedance occurred over the testing period, signifying that the coating had undergone little water uptake.

Also serving as references were two coated 1" × 6" panels, which were tested under extreme environmental conditions; one at high temperature and humidity (Panel #4), and one at low temperature and humidity (Panel #5). The low-frequency impedance spectra for Panel #4 demonstrates that the coating did not perform well in high temperature and humidity conditions (65°C, 98% RH). Blisters began to form within five days of exposure and the impedance spectra confirmed the degradation. Panel #5 performed well at low temperatures (0°C). The low-frequency impedance spectra indicated very little water uptake throughout the extent of testing.

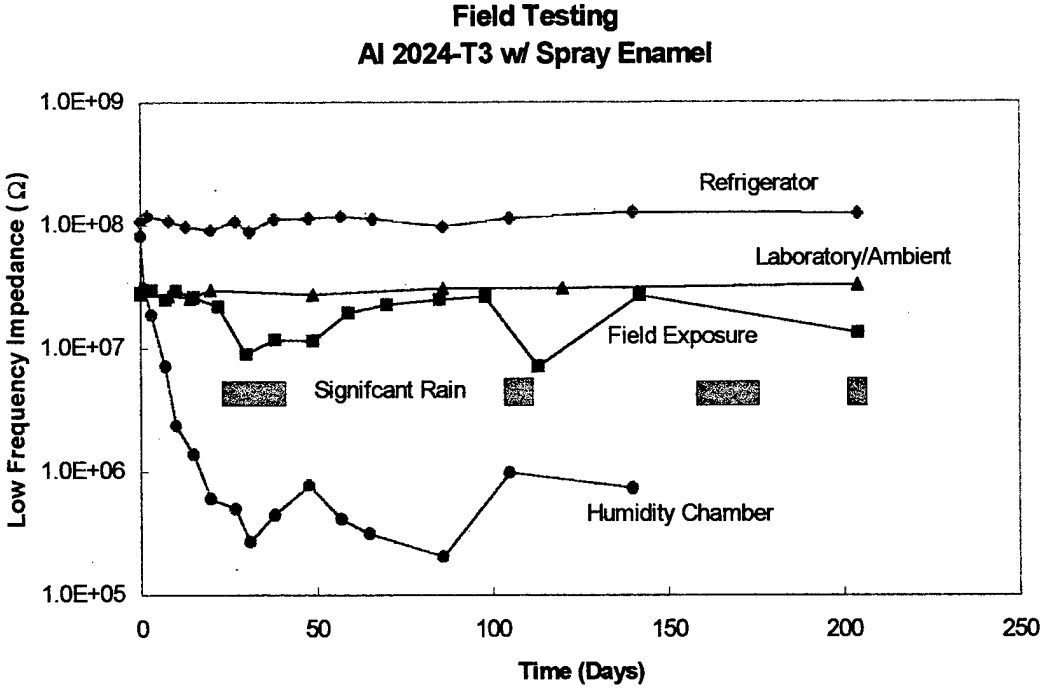

Figure 24. *Low Frequency Impedance of Field Testing Panels.*

Task 7. Design and Fabrication of Upscale Prototype Sensor.

The upscale prototype hand-held sensor was fabricated with the sensing component encased in a PVC shell (Figure 25). The circular base of the sensor was also constructed of PVC and was sized to allow the sensor to be held by the fingertips or in a manner similar to a joystick.

Figure 25. *Upscale Prototype Sensor.*

Task 8. Testing of Upscale Prototype Sensor.

Measurements taken with the upscale sensor were comparable to the first prototype sensor (Figure 26). No problems existed when measuring low impedances at all frequencies (i.e., samples with defects), but higher impedances (at low frequencies) showed some fluctuation. The major problems with the upscale sensor involved operation. It was awkward and tiring to hold for an extended period of time. The ratio of the areas of the fingertip base to the sensing component was too large, which made it tend to rock when holding. The handle was too short, which made it very difficult to hold like a joystick and presented some minor congestion between the user's hand and the wire connections. Vertical and over-head surfaces were virtually impossible to test due to hand fatigue.

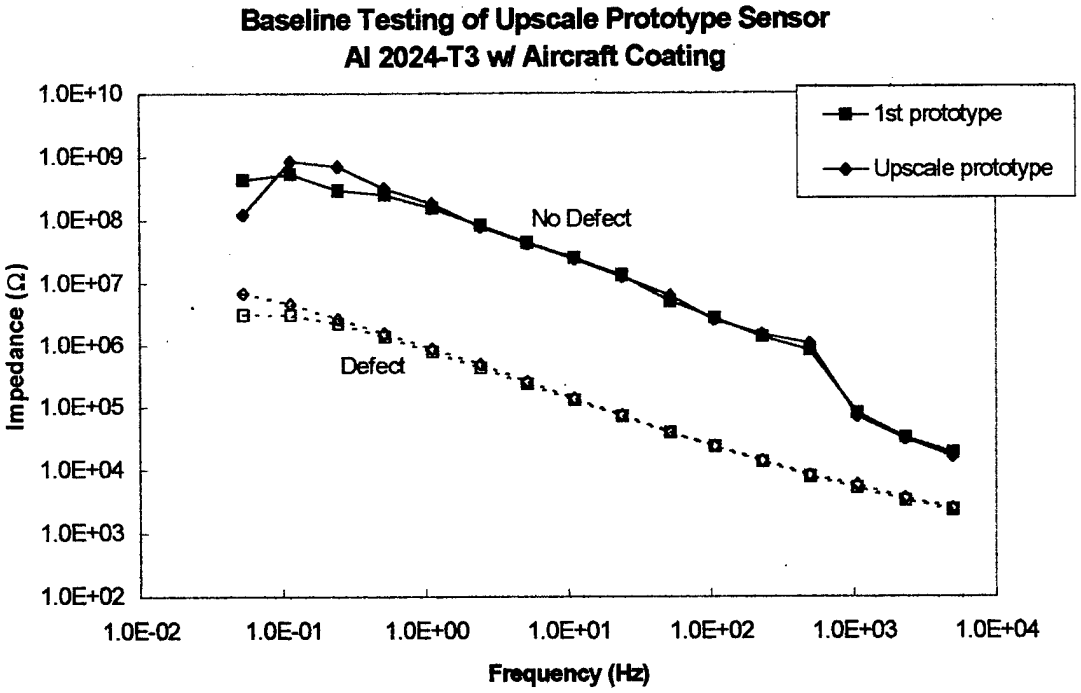

Figure 26. *Baseline Upscale Prototype Sensor Testing.*

Task 9. Final Prototype Sensor Development.

The final prototype sensor (Figure 3) was designed to provide easier use than the upscale sensor. It had a much smaller diameter and was several inches longer. A long shielded lead wire was permanently attached. This allowed the connection to the Gamry to be made at a distance from the sensor, thus eliminating the wire congestion around the sensor. The connection to the Gamry was made with a BNC connector. The sensor was intended to be used like a pen-type probe. The final sensor was much easier to use and provided results similar to both the first prototype sensor and the upscale sensor (Figure 27).

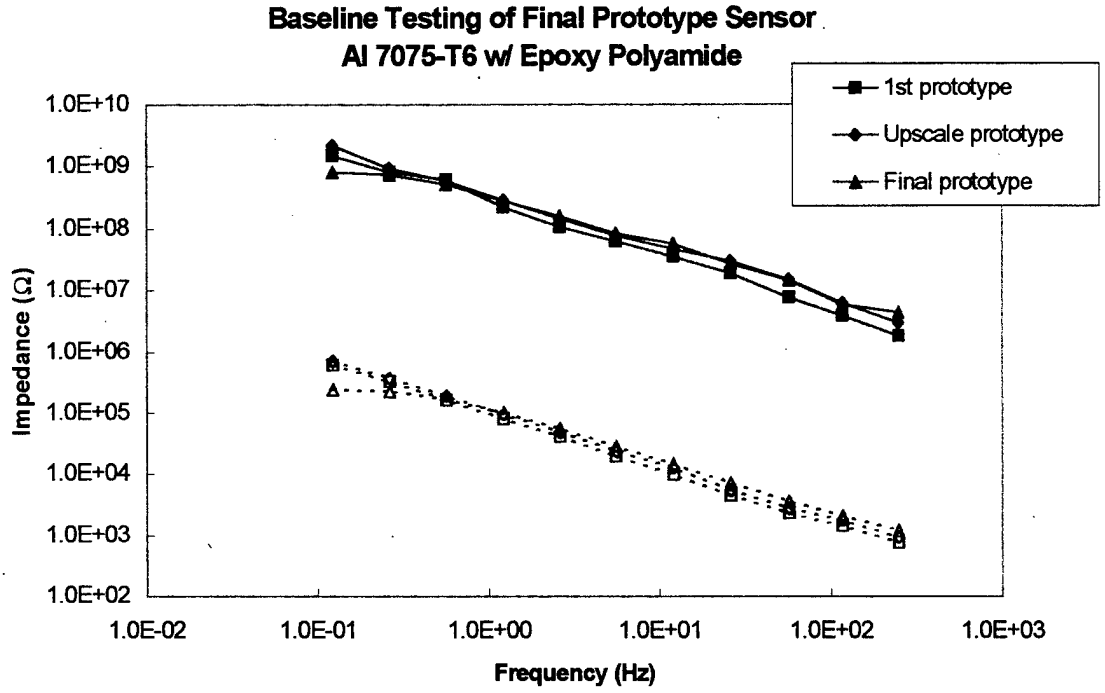

Figure 27. *Baseline Testing of Final Prototype Sensor.*

Task 10. Testing of the Final Prototype Sensor.

Some difficulties with high impedance interference were encountered with this sensor and the previous prototypes. Extensive testing was conducted to determine the cause of the interferences at high impedances. The problem results from the very small current magnitudes required for the high impedance measurements. The test currents are so small that they are susceptible to even the slightest interferences (noise) in the testing environment. The EG&G laboratory units do not appear to be as susceptible to interferences as the Gamry portable unit. When the experiments with the Gamry unit were run in a closed environment, the plots showed no interference. To enhance the performance in the presence of laboratory noise, a Faraday shield was used. The quality of the impedance plots improved with the shield in place (Figure 28). Field testing provided further challenges because the use of a Faraday shield was impractical. Three possible sources of interference were identified; the sensor, the substrate, or the Gamry unit. The final sensor is constructed with a shielded cable and has a very small sensing element. Therefore, it is unlikely that the sensor would pick up interferences, even being operated in a hand-held manner.

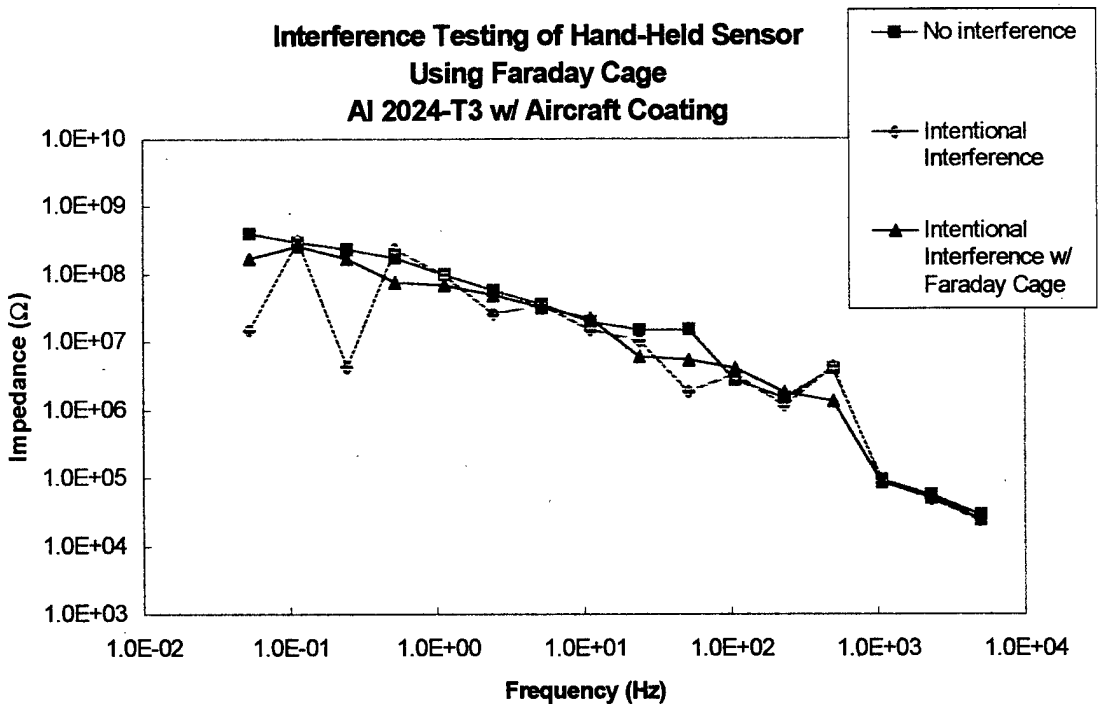

Figure 28. *Interference Testing of Final Prototype Sensor.*

As part of the testing of the final sensor, demonstrations were held at Warner Robins Air Force Base in Georgia, and Tinker Air Force Base in Oklahoma. These demonstrations were extremely valuable to the project and the continued development of the the sensor. Accomplishments of these trips were:

- Demonstrated effectiveness of the hand held sensor in inspecting aircraft for corrosion and coating degradation.
- Began to build impedance database of actual aircraft coatings for continued development of DSI's analysis software.
- Received feedback from those more closely involved in aircraft corrosion and aircraft maintenance protocols.
- Recognized the need to make the system more portable, with the use of a batteries, for efficient field testing.
- Recognized the need to shorten the testing period.
- Recognized the need to continue to evaluate the effects of interference on the impedance spectra.

The most valuable testing was conducted on aircraft samples provided by both Warner Robins and Tinker because it allowed the first testing of actual aircraft parts. DSI was able to make some EIS measurements on the following aircraft parts:

- 707 Fuselage
- C130 Fuselage, Elevator Rudder, Aterons, Inboard Flap
- F15 Pylon Tank, Horizontal Stabilizer
- C141 Pedal Door
- C135 Fuselage

Figure 29 shows impedance curves measured for the C130 fuselage and the 707 fuselage tested at Warner Robins. The C130 measurements were taken on different layers of paint (white and blue), while the 707 measurements were taken on regions of differing visible degradation. The impedance of the two C130 coatings was nearly identical and was very high, signifying a good coating. The 707 impedance measurements indicated a clear difference between the good and bad regions of testing. The region that showed a visible defect had low frequency impedances near 10^7 Ω, while the region without defects had a low frequency impedance over 10^9 Ω. Figures 30 through 33 show photographs of the use of the corrosion sensor on various aircraft parts.

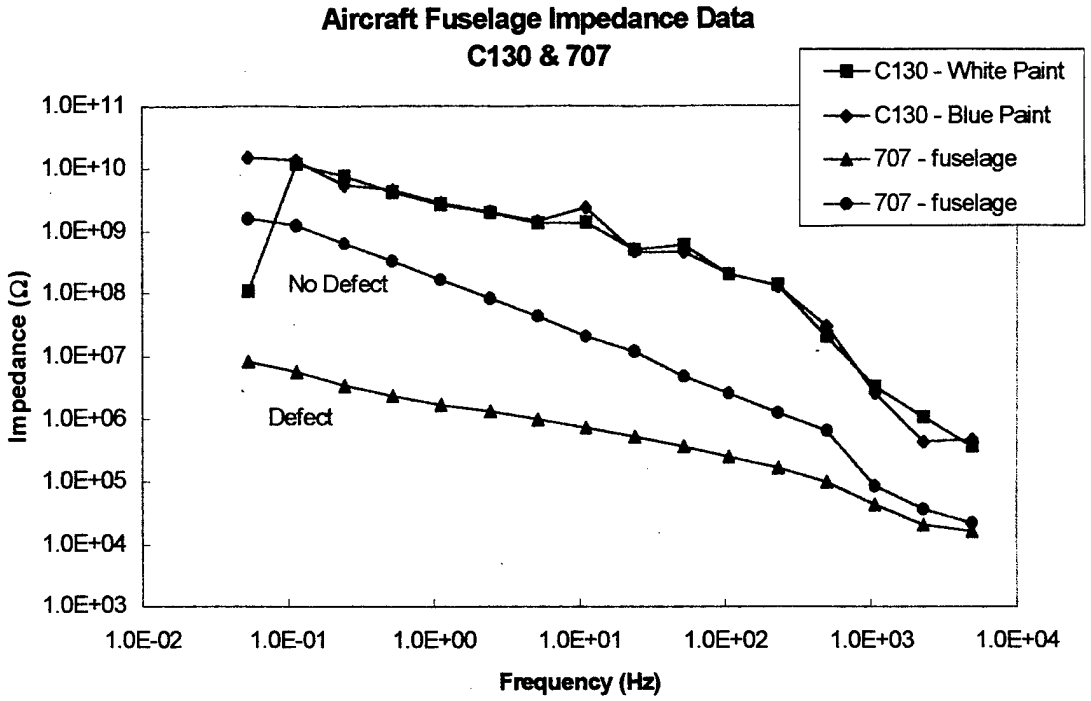

Figure 29. ***Impedance Spectra of Aircraft Parts.***

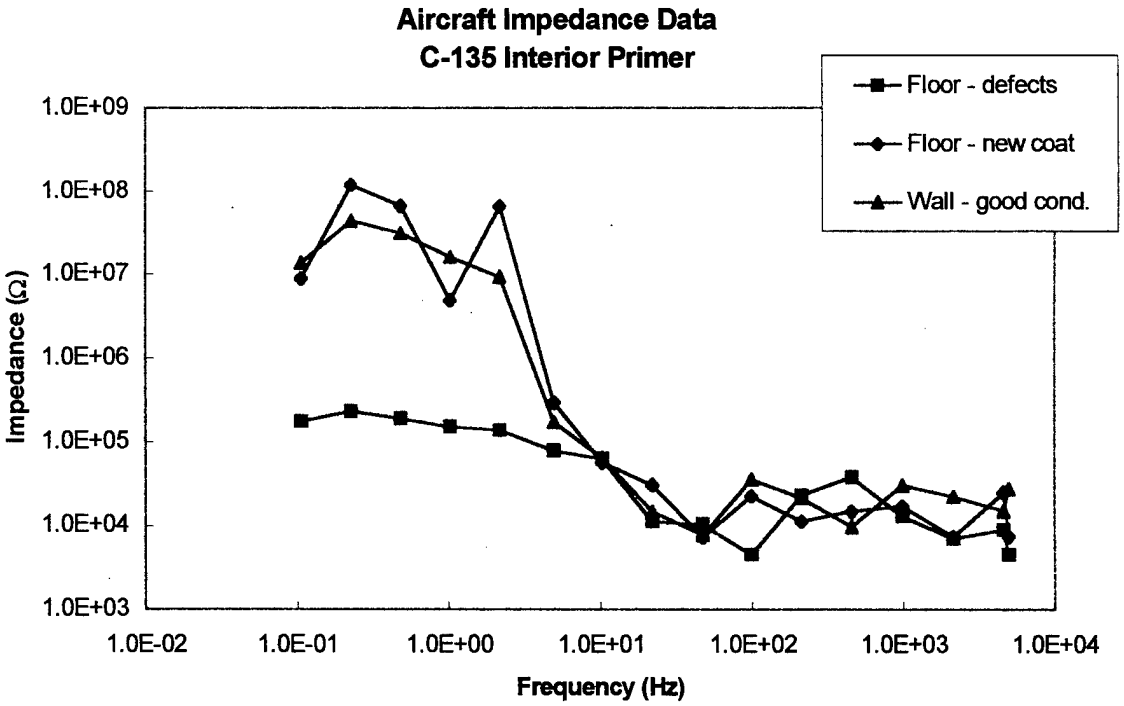

Figure 30. ***Impedance Spectra of C-135 Aircraft Parts.***

Figure 31. *Photograph of Testing on C130 Fuselage.*

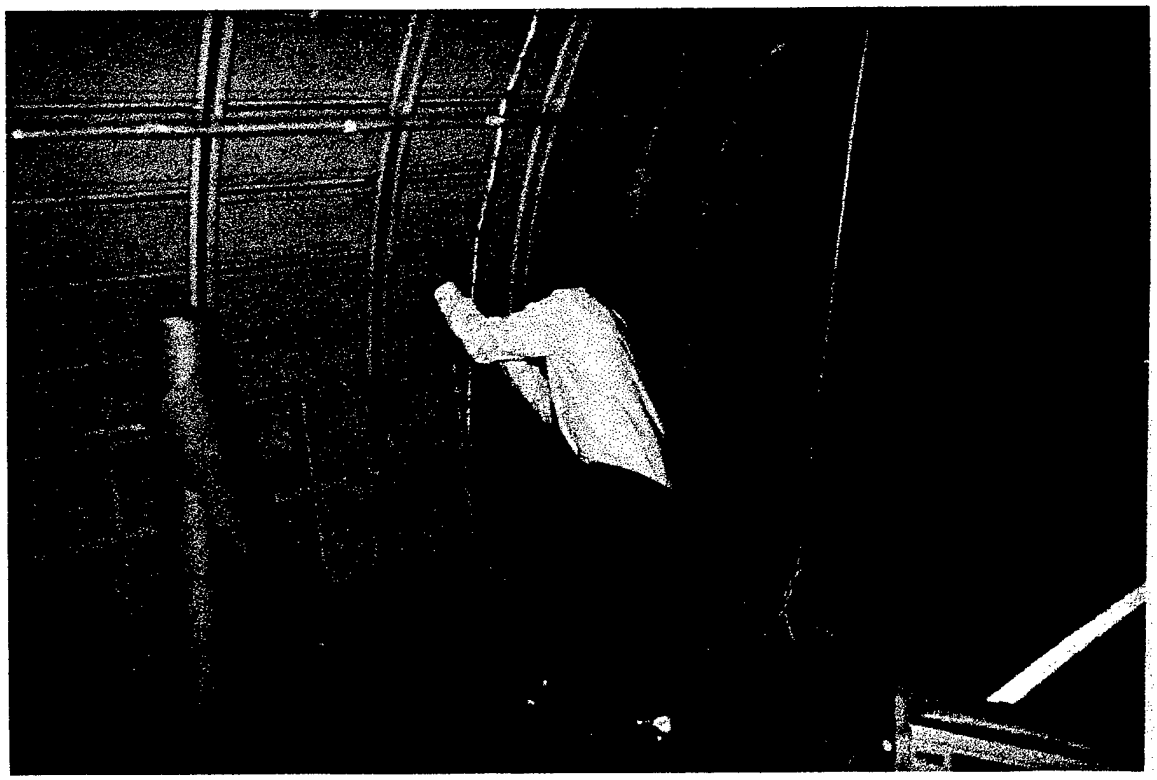

Figure 32. *Photograph of Testing on C-135.*

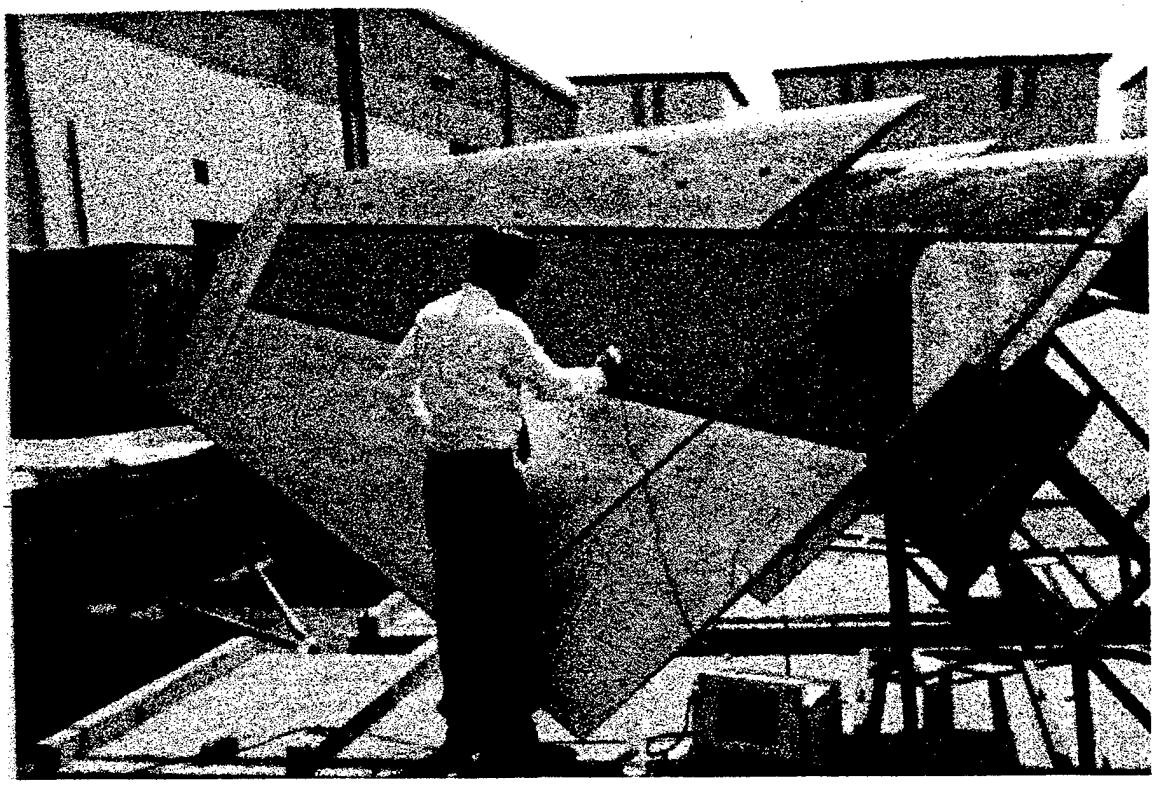

Figure 33. *Photograph of Testing on F15 Horizontal Stabilizer.*

Figure 34. *Photograph of Testing on C130 Elevator Rudder.*

Task 11. Incorporate Sensor into Aircraft.

A preliminary design to incorporate the conductive ink electrodes into new or existing aircraft is included in Figure 34 and is similar to that proposed in Reference 20. The placement of the electrodes will allow inspectors to monitor locations otherwise difficult to access. The leads from the sensors can be terminated at a central location to allow for expedient testing. Determination of the final location of the sensors will depend on the individual aircraft designs, and the corrosion problems associated with each.

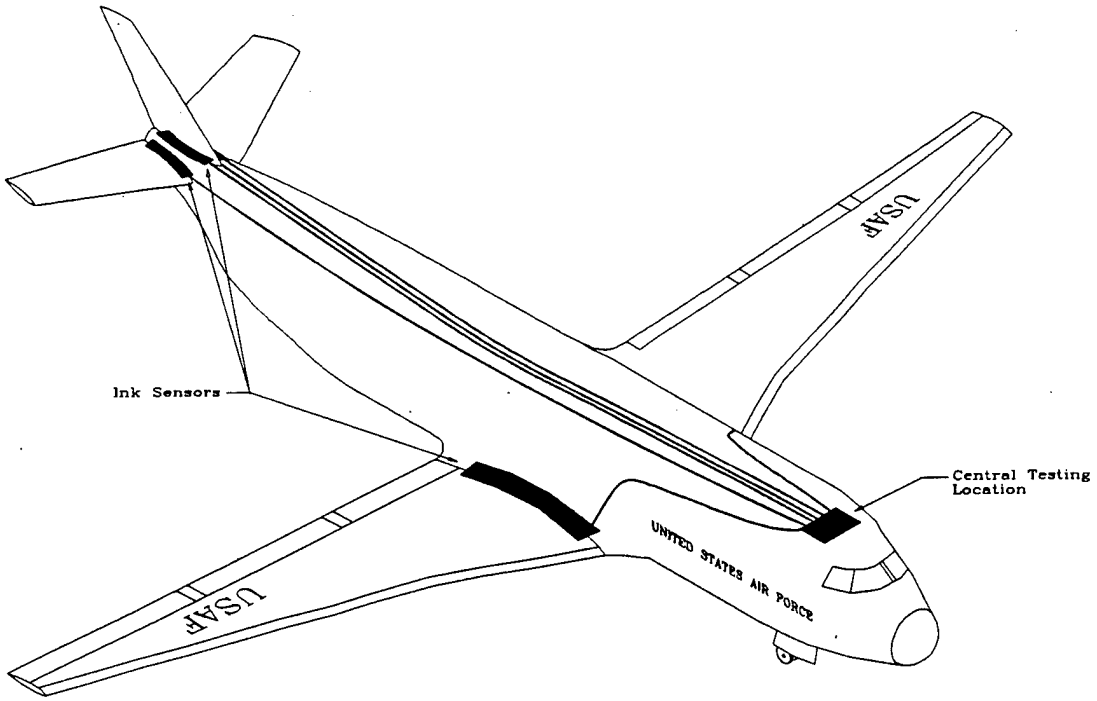

Figure 35. *Placement of In-situ Sensors on Aircraft.*

PERSONNEL SUPPORTED:

This program involves a collaborative effort between Dr. Chester Dacres, Dr. Guy Davis, Dr. Lorrie Krebs, Mark Shook, Duane Stewart, Brian Taggart, and Bridget Wenner of DACCO SCI, INC., who collectively have many decades of experience in corrosion, polymer/metal interfaces, and instrumentation. Each investigator brings a specific expertise to the program that is critical to its success. Dr. Dacres has over 25 years of experience in corrosion systems, electrochemical systems and sensor development for U.S. Navy ships and underground storage tanks. Dr. Davis has applied electron and photon spectrometric and electrochemical techniques to the analysis of surface, interface, thin film, and coatings in corrosion, battery, and adhesion applications for 15 years. He was one of the developers of the existing laboratory version of the in-situ corrosion monitor.

Individual program responsibilities are listed below:

• Monitor optimization	Dr. Dacres, Dr. Davis, Dr. Krebs, Mr. Shook, Mr. Taggart, Ms. Wenner
• Environmental testing	Dr. Dacres, Dr. Davis, Dr. Krebs, Mr. Shook, Mr. Stewart, Mr. Taggart, Ms. Wenner
• Reporting	Dr. Dacres, Dr. Davis, Dr. Krebs, Mr. Shook

PUBLICATIONS:

A paper discussing the research performed in the Phase I project has been completed and published by the American Society of Mechanical Engineers (ASME) as part of the journal for the ASME 1995 Winter Annual Meeting.

INTERACTIONS / TRANSITIONS:

a. <u>Participation/presentations at meetings, conferences seminars, etc</u>.

1. "The Use of Electrochemistry and Ellipsometry for Identifying and Evaluating Corrosion on Aircraft," <u>C.M. Dacres</u>, C.R. Anderson, B.C. Taggart, and P.L. Whisnant, AFOSR Surface Science and Molecular Dynamics Contractors' Conference (Washington D.C., October 22-24, 1995).

2. "The Use of Electrochemistry and Ellipsometry for Identifying and Evaluating Corrosion on Aircraft," C.M. Dacres, C.R. Anderson, <u>B.C. Taggart</u>, and P.L. Whisnant, Symposium on Structural Integrity in Aging Aircraft, 1995 ASME Meeting (San Francisco, CA, November 16, 1995).

3. "Monitoring Adhesive Bond and Coating Integrity with Electrochemical Impedance Spectroscopy," G.D. Davis, C.M. Dacres, B.C. Taggart, B.S. Wenner. and P.L. Whisnant, 41st Inter. SAMPE Symp. (Anaheim, CA, March 1996).

4. "Monitoring Adhesive Bond and Coating Integrity with Electrochemical Impedance Spectroscopy," G.D. Davis, C.M. Dacres, B.C. Taggart, B.S. Wenner, and P.L. Whisnant, 4th Inter. Conf. on Adhesion and Surface Analysis, (Loughborough, UK, April 1996).

5. "X-ray Photoelectron Spectroscopy, Auger Electron Spectroscopy, and Secondary Ion Mass Spectrometry," G.D. Davis, ASM Inter. Educational Symp. (Oak Ridge, TN, April 1996) (INVITED).

6. "Development of an Electrochemical Sensor to Detect Corrosion of Aging Aircraft," G.D. Davis, C.M. Dacres, B.C. Taggart, B.S. Wenner, and M. Shook, AeroMat'96: 7th Annual Advanced Aerospace Materials and Processes Conf. & Exposition, (Dayton, OH, June 1996).

7. "Development of an Electrochemical Sensor to Detect Corrosion of Aging Aircraft," C.M. Dacres, G.D. Davis, B.C. Taggart, B.S. Wenner, and M. Shook, AeroMat'96: Air Force 4th Aging Aircraft Conf., (Colorado Springs, CO, July 1996).

8. "Monitoring Coating and Bondline Integrity with an In-Situ Corrosion Sensor," G.D. Davis, Gordon Research Conference on the Science of Adhesion (Tilton, NH, August 1996) (INVITED).

9. "Electrochemical Sensors for Evaluating Corrosion and Adhesion on Painted Metal Structures," G.D. Davis, Ford Motor Company (Dearborn, MI, October 1996). (INVITED).

10. "Electrochemical Sensors for Evaluating Corrosion and Adhesion on Painted Metal Structures," G.D. Davis, 3M Corporation (Minneapolis, MN, May 1997). (INVITED).

b. Consultative and advisory functions.

1. Courtaulds Aerospace, Inc. of Berekely, CA has been used as a consultative source for aircraft coatings for U.S. Air Force aircraft and has provided preparation of test samples for Phase II testing that meet military specifications.

2. ISPA has provided test samples coated with high performance fluoropolymer coatings, typically used in the chemical industry, for EIS analysis with the sensors.

c. **Transitions.**

In view of the tremendous economic and environmental cost of aircraft maintenance, the potential commercial applications of this technology are enormous. The specific techniques, which will be developed, will be of greatest use in quality control applications and in accelerated testing of materials systems in realistic atmospheres with common pollutants so that better corrosion-resistant materials can be developed as a spin-off. In addition, aircraft will have an increased lifetime utility with lowered lifetime maintenance costs. The commercial ramifications of electrochemical corrosion sensor development are obvious to the military and the aircraft industry, as well as to the insurance industry where the potential economic benefits could be substantial. Additionally, increased aircraft safety will be one of the most important benefits of this new technology.

In addition to uses in the aviation industries, this corrosion detector will have spin-off applications for the detection of corrosion in bridges, automobiles and trucks, chemical plants, pipelines and storage tanks. The sensor will also greatly facilitate development of new coatings by providing a direct comparison of degradation occurring during accelerated laboratory testing and ambient service conditions.

To this end, DACCO SCI, INC. has entered into three Phase III programs with companies in the aerospace, automotive, and coatings industries to help screen or develop new, high-performance coatings.

NEW DISCOVERIES, INVENTIONS, OR PATENT DISCLOSURES:

Preparations for a patent for the hand-held sensor to be developed in the Phase II effort are currently underway.

HONORS / AWARDS:

Chester M. Dacres, Ph.D., P.E.
Principal Investigator

1986 Bernard Smith Award

Guy D. Davis, Ph.D.
Associate Investigator

1996 Adhesion Society - Robert L. Patrick Fellow

1996 Adhesion Society - President

1996 American Vacuum Society - Fellow

1986 Distinguished Young Scientist Award of the Maryland Academy of Sciences

REFERENCES:

1 USAF 1994 Scientific Advisory Broad Summer Study on Life Extension and Capability Enhancement of Existing Air Force Aircraft.

2 R.C. Kinzie, "The Cost of USAF Corrosion Maintenance," *Aerospace Corrosion Control 1992,* 1992.

3 D.W. Hoeppner, L. Grimes, A. Hoeppner, J. Ledesma, T. Mills, and A. Shah, "Corrosion and Fretting as Critical Aviation Safety Issues: Case Studies, Facts, and Figures from US Aircraft Accidents and Incidents," *Proc. 18th Symp. Inter. Comm. on Aeronautical Fatigue* (Melbourne, Australia, May 1995), p. 87.

4 C.I. Change, "Aging Aircraft Science and Technology Issues and Challenges and USAF Aging Aircraft Program," in *Structural Integrity in Aging Aircraft* **AD-47** ed., C.I. Chang and C.T. Sun, (ASME, New York, 1995), p. 1.

5 F. Mansfeld, "Recording and Analysis of AC Impedance Data for Corrosion Studies: I. Background and Methods of Analysis," *Corrosion* **37**, 301 (1981).

6 M. Kendig, F. Mansfeld, and S. Tsai, "Determination of the Long Term Corrosion Behavior of Coated Steel with AC Impedance Measurements," *Corros. Sci.* **23**, 317 (1983).

7 M. Kendig and J. Scully, "Basic Aspects of the Application of Electrochemical Impedance for the Life Prediction of Organic Coatings on Metals," *Corrosion89* Paper 32, NACE (1989).

8 J.R. Scully, "Electrochemical Impedance of Organic-Coated Steel: Correlation of Impedance Parameters with Long-Term Coating Deterioration," *J. Electrochem. Soc.* **136**, 979 (1989).

9 W.S. Tait, *J. Coat. Technol.* **61**, 57 (1989).

10 J.N. Murray and H.P. Hack, "Long Term Testing of Epoxy Coated Steel in ASTM Sea Water Using EIS," *Corrosion90* Paper 140, NACE 1990.

11 J.A. Grandle and S.R. Taylor, "Electrochemical Impedance Sprectroscopy of Coated Aluminum Beverage Containers: Part 1 – Determination of an Optimal Parameter for Large Sample Evaluation," *Corrosion* **50**, 792 (1994).

12 A. Zdunek and X. Zhan, "A Field EIS Probe and Methodology for Measuring Bridge Coating Performance," *4th World Congress on Coating Systems for Bridge and Steel Structures,* Steel Structures Painting Council, St. Louis, MO, February 1995.

13 K. Homma et al., "Utilization of Electrochemical Impedance Techniques to Estimate Corrosion Damage of Steel Infrastructure," *Corrosion Forms and Control for Infrastructure,* ASTM STP 1137, Victor Chaker, ed., ASTM, Philadelphia, 1992.

14 P.C. Su, O.F. Devereux, and W. Madych, "Impedance Imaging for Prediction and Detection of Airframe Corrosion," *Structural Integrity in Aging Aircraft,* AD-Vol. 47, C.I. Chang, and C.T. Sun, ed., American Society of Mechanical Engineers, 1995.

15 T.C. Simpson, P.J. Moran, W.C. Moshier, G.D. Davis, B.A. Shaw, C.A. Arah and K.L. Zankel, "An Electrochemical Monitor for the Detection of Coating Degradation in Atmosphere," *J. Electrochem. Soc.* **136**, 2761 (1989).

16 T.C. Simpson, P.J. Moran, H. Hampel, G.D. Davis, B.A. Shaw, C.A. Arah, T.L. Fritz, and K.L. Zankel, "Electrochemical Monitoring of Organic Coating Degradation during Atmospheric or Vapor Phase Exposure," *Corros.* **46**, 331 (1990).

17 T.C. Simpson, H. Hampel, G.D. Davis, C.O. Arah, T.L. Fritz, P.J. Moran, B.A. Shaw, and K.L. Zankel, "Evaluation of the Effects of Acidic Deposition on Coated Steel Substrates," *Prog. Organic Coatings* **20**, 199 (1992).

18 V.S. Agarwala, "In-Situ Corrosivity Monitoring of Military Hardware Environments," *Corrosion96* Paper 632, NACE 1996.

19 R.G. Kelly, S.H. Jones, W. Blanke, J. Aylor, and A. Batson, "Embeddable Microinstruments for Corrosion Monitoring," *Corrosion97* Paper 294, NACE 1997.

20 P.R. Roberge, M.A.A. Tullmin, L. Genier, C. Ringas, "Corrosion Surveillance for Aircraft," *Materials Performance* **35**, No. 7, 50 (1996).